Title: Flattened circadian glucocorticoid oscillations cause obesity due to increased lipid turnover and lipid uptake

Authors: Stefan Tholen[1], Kyle M. Kovary[1], Atefeh Rabiee[1], Ewa Bielczyk-Maczyńska[1], Wenting Yang[1] and Mary N. Teruel[1,2*]

Affiliations:
[1]Department of Chemical and Systems Biology, Stanford University, Stanford, CA, 94305, USA.
[2]Department of Biochemistry and the Drukier Institute of Children's Health, Weill Cornell Medicine, NY, NY 10065, USA.

[*]**Corresponding Author and Lead Contact:** mnt4002@med.cornell.edu

ABSTRACT

Chronic stressors flatten circadian glucocorticoid (GC) oscillations, which has been correlated with negative health outcomes including obesity. How such flattened circadian GC oscillations affect metabolism and fat storage remains unknown. Here we investigated the consequences in mice and found that flattening of GC oscillations results not only in body weight gain, mainly due to increases in white fat depot mass, but also leads to hyperinsulinemia and fat accumulation in brown adipose tissue. A transcriptomic analysis of white and brown adipose tissues revealed that flattened GC oscillations cause dysregulated lipid metabolism with a prominent role of the fatty acid transporter Cd36. Indeed, *Cd36* knockout mice are partially protected against the adverse effects of flattened GC oscillations including body weight gain and lipid accumulation in the brown and visceral white fat depots. These results provide insights on how conditions associated with flattened GC levels cause obesity.

KEYWORDS

Obesity, stress, circadian rhythm, hormone oscillations, glucocorticoids, brown adipose tissue, white adipose tissue, lipid metabolism, Cd36

HIGHLIGHTS

- Flattening of circadian GC oscillations in mice, despite keeping mean circulating GC levels the same, results in body weight gain, lipid accumulation in both brown and white adipose tissues (BAT and WAT), and hyperinsulinemia.

- Markedly, flattening GC oscillations for short periods of three days is sufficient to increase lipid accumulation and mass in BAT, but longer periods are needed to increase lipid accumulation and mass in WAT.

- Transcriptomics analysis shows increased expression of a key regulator of fatty acid uptake, CD36, and knockout of CD36 partially protects cells from flattening GC oscillations

INTRODUCTION

In healthy mammals, glucocorticoids (GCs) are secreted in circadian oscillations that are low during sleep and peak before awakening (Weitzman et al., 1971). These circadian oscillations of GCs have been shown to be essential for normal body function since GCs provide wake-up and other essential timing signals (Oster et al., 2006). Secretion of GCs is controlled by the hypothalamic-pituitary-adrenal (HPA) axis, which responds strongly to stress. A state of chronic stress, such as occurs from depression, jet lag, irregular eating and sleeping schedules, can flatten the normal circadian glucocorticoid oscillation pattern, meaning that the GC peak levels are decreased and trough levels are elevated but the daily mean values do not significantly change (Adam, 2017; Dallman et al., 2000; Miller et al., 2007). A growing body of evidence supports that flattening GC levels, and not only excessive amounts of GCs, can lead to disease. For example, flattened GC oscillations resulting from depression, jet lag, irregular eating and sleeping cycles, aging, or prolonged treatment with GCs have been shown to closely correlate with obesity (Adam, 2017; Broussard and Cauter, 2016; Dallman et al., 2000; Doane et al., 2013).

Our goal was to understand the basis and physiological consequences of the fat mass increases that we previously observed in response to flattening of daily physiological levels of GCs (Bahrami-Nejad et al., 2018). Whereas increased GC levels have been shown to promote the the development of obesity (Lee et al., 2014; Peckett et al., 2011), most *in vivo* studies administrated high pharmacological doses of GCs which does not provide insight into how variations in normal physiological levels of GCs – such as are seen in chronic stress, jet lag, night shift work - affect body metabolism (Adam, 2017; Lee et al., 2014; Lightman and Terry, 2014; Miller et al., 2007). Previous studies observed that GC-mediated increases in fat pad size are associated with both an increased number of adipocytes (hyperplasia) and an increased cell volume (hypertrophy) (Campbell et al., 2011; Lee et al., 2014; Rebuffé-Scrive et al., 1992). In previous work, we demonstrated that flattening of normal circadian GC oscillations in mice results in significant body weight gain and a more than two-fold expansion of the white adipose tissue (WAT) depots in mice within 26 days (Bahrami-Nejad et al.,

2018). We found that the expansion of the subcutaneous WAT was exclusively caused by an increase in cell volume whereas expansion of the visceral WAT (vWAT) was characterized by both an increase in cell volume and an increased number of adipocytes. We demonstrated that the increased adipogenesis in the vWAT when the daily circadian GC oscillation pattern was flattened was due to preadipocytes having a slow and fast positive feedback circuit centered on PPARG, the main transcriptional regulator of adipogenesis. Whereas our previous study provided a molecular explanation of the increased adipogenesis observed in the vWAT when GC oscillations were flattened, the molecular mechanism underlying the significant increase in cell volume in the visceral and subcutaneous fat depots upon flattening GC remained elusive.

In this study we carried out a timecourse analysis over 4 weeks in mice to better understand how and when obesity develops when GCs are flattened. As in our previous study (Bahrami-Nejad et al., 2018), we found that flattening of circadian GC oscillations results in body weight gain primarily due to increases of the WAT depots. We went on to show that flattening of GC oscillations leads to hyperinsulinemia, as well as to significant lipid accumulation in brown adipose tissue (BAT) within 3 days, which precedes the lipid accumulation and expansion of the white adipose tissue (WAT) that occurs only days later. Global analysis of the transcriptome of WAT and BAT revealed alterations in gene expression dependent on flattened GC oscillations and point to increased lipid turnover and lipid uptake in both fat depots. Taken together, our findings demonstrate that flattened circadian GC oscillations results in significant overall weight gain primarily due to lipid accumulation in WAT and BAT, which in turn is caused by a simultaneous increase in lipid uptake, as well as in synthesis and breakdown of triglycerides (TG). Furthermore, our study identified genes whose expression is sensitively regulated by flattening of circadian GC oscillations such as the fatty acid transporter Cd36 which was upregulated in WAT and BAT. The importance of Cd36 for lipid accumulation was highlighted by our experiments in *Cd36* knockout mice, which proved to be partially protected against body weight gain and lipid accumulation in visceral WAT and BAT induced by flattening of GC oscillations. Furthermore, the transcriptomic analysis in this study identified a set of genes in addition

to *Cd36*, whose expression in BAT and vWAT is regulated by GC flattening and that may also be targets that can be regulated therapeutically to prevent the unwanted obesity that can occur in response to chronic stress and other physiological conditions in which GCs are flattened.

RESULTS

Flattening of daily corticosterone oscillations in mice results in lipid accumulation in white adipose tissue.

To investigate the effect of flattening daily glucocorticoid levels at physiological GC levels, we implanted corticosterone pellets subcutaneously in C57BL/6J male mice. The pellets released corticosterone at a concentration that flattened circulating corticosterone oscillations, but kept mean corticosterone levels close to normal physiological levels (Bahrami-Nejad et al., 2018; Hodes et al., 2012). Hence, mice implanted with corticosterone pellets showed increased corticosterone levels in the nadir of the diurnal corticosterone pattern while also decreasing corticosterone at the peak time in the evening compared to sham pellet-implanted mice **(Figure 1A)**. Confirming the results of our previous study (Bahrami-Nejad et al., 2018), mice with flattened corticosterone oscillations increased their body weight faster than sham pellet-implanted mice and ended up weighing 9.1% more after 21 days **(Figure 1B)**. Interestingly, as was found in our previous study (Bahrami-Nejad et al., 2018) and in other studies which administered sustained GCs longterm (Bowles et al., 2015; Luijten et al., 2019), the increased weight gain cannot be explained by higher food intake **(Figure 1C)**, and a reduction in metabolism may be a more significant contributing factor.

To test whether corticosterone pellet-implanted mice gain weight mainly by expansion of the white fat depots, the subcutaneous inguinal WAT and the visceral epididymal WAT were dissected and weighed. Located under the skin, the inguinal WAT is the main subcutaneous WAT depot (Chusyd et al., 2016) , and we will refer to it as sWAT throughout this study. The epididymal WAT that surrounds the gonads represents the major visceral WAT depot (Chusyd et al., 2016), and we will refer to it as vWAT throughout this study. In general, a stronger expansion was observed for the vWAT, which

expanded 3-fold in 21 days, whereas the weight of the sWAT increased slightly more than 2-fold. Both WAT depots showed a significant increase in weight already after 7 days of flattening corticosterone oscillations **(Figure 1D-G)**. This early expansion of the white fat depots was confirmed by hematoxylin and eosin (H&E) staining of sWAT and vWAT which revealed increased cell volumes of the adipocytes in both fat depots from day 7 **(Figure 1H/J)**. The cell volume increases are quantified in **Figure 1I/K**.

Increasing the peak amplitudes of corticosterone does not result in lipid accumulation in the white fat depots

To test whether the lipid accumulation in the white fat depots shown in **Figure 1** is due to flattening of diurnal corticosterone levels and not caused by the amount of corticosterone released by the corticosterone pellet, we injected the mice at 5 PM each day for 21 days with the same total amount of corticosterone that is released by the corticosterone pellet in one day. This injection resulted in a more than 10-fold increase in the daily peak amplitude of corticosterone **(Figure 2A)**. Strikingly, corticosterone-injected mice did not show a significant increase in body weight compared to sham-injected control mice **(Figure 2B).** Furthermore, their food intake was not altered **(Figure 2C).** In addition, no differences in fat pad weight were detected between the sWAT **(Figure 2D/E)** and vWAT of the corticosterone- and sham-injected mice **(Figure 2G/H)**, and histological analysis of the tissues showed no differences in lipid accumulation **(Figure 2F/I)**.

Taken together, our results show that increasing the peak amplitude of corticosterone in the evening phase did not affect body weight gain or lipid accumulation in the white fat depots. Hence as we had previously shown (Bahrami-Nejad et al., 2018), short spurts of glucocorticoids do not seem to promote weight gain as long as the increase in glucocorticoids occurs during the time window that glucocorticoids are normally high and sufficiently long off-periods with low glucocorticoid levels are maintained (Dallman et al., 2000). The fact that corticosterone pellet-implanted mice and corticosterone injected mice received the same amount of corticosterone per day and only the pattern of the diurnal corticosterone levels as measured in blood serum differed **(Figure 1A/2A)**, showed that

flattening of diurnal corticosterone levels is indeed responsible for the body weight gain and lipid accumulation in the white fat depots **(Figure 1)**.

Flattening of daily corticosterone oscillations in mice results in lipid accumulation in brown adipose tissue (BAT)

BAT is a specialized organ that uses carbohydrates and fat as resources to produce thermal energy needed to regulate body temperature (Cannon and Nedergaard, 2004). In rodents, expansion of BAT or increasing its respiratory activity has shown to be protective against metabolic diseases and obesity (Feldmann et al., 2009). With the discovery of thermogenic brown adipocytes in humans (Cypess et al., 2009; Saito et al., 2009; Van Marken Lichtenbelt et al., 2009), BAT expansion or boosting its respiratory activity has gained significant attention as a therapeutic treatment for obesity and related disorders (Betz and Enerbäck, 2015; Harms and Seale, 2013; Kusminski et al., 2016; Sidossis and Kajimura, 2015). Numerous studies showed that GC treatment in rodents can lead to accumulation of lipids in the brown fat depot (Ketzer et al., 2019; Luijten et al., 2019; Shen et al., 2017; Strack et al., 1995).

To test if flattening of diurnal corticosterone oscillations without increasing the total corticosterone amount per day is already sufficient to cause lipid accumulation, we analyzed BAT of corticosterone and sham pellet-implanted mice. Indeed, flattening diurnal corticosterone oscillations resulted in an increase in BAT size **(Figure 3A)** and a 3-fold increase in organ weight **(Figure 3B)**. This was confirmed by histological analysis of BAT, where larger lipid-filled adipocytes could be detected. **(Figure 3C**, quantified in **Figure 3D)**. The lipid droplets were characterized by a shift from a multilocular to a more unilocular morphology, giving the tissue a “whitened” appearance. As observed for the white fat depots, injection of the same corticosterone amount released by the corticosterone pellet per day increased the peak amplitude in the evening/waking phase but did not affect BAT tissue size **(Figure 3E/F)**. In line with this observation, histological analysis of BAT did not reveal any morphological changes between mice subcutaneously injected with corticosterone and mice injected

with the solvent control **(Figure 3G)**. As shown for WAT, it is not the amount of corticosterone given to the mice once per day via injection or via pellet implantation that causes lipid accumulation in the fat tissue. Rather, it is the loss of the off-period in the corticosterone oscillations that promotes fat deposition in WAT and BAT. Interestingly lipid accumulation in BAT was already detected 3 days after corticosterone pellet implantation preceding lipid accumulation in subcutaneous and visceral WAT, which was first detected 7 days after pellet implantation **(Figure 1E/G)**. Taken together, our results show that BAT reacts more sensitively and rapidly to flattening of corticosterone oscillations than the white fat depots analyzed in this study.

Flattening of daily corticosterone oscillations in mice does not result in hyperlipidemia or fat deposition in the liver

Rodents treated with chronic high concentrations of corticosterone have been shown to rapidly increase body weight due to expansion of the fat depots (Bowles et al., 2015; Campbell et al., 2011; Chimin et al., 2014; Karatsoreos et al., 2010). Often the expansion of fat depots is accompanied by fat deposition in the liver, an increase of triglycerides in blood plasma, and insulin resistance (Bowles et al., 2015; Campbell et al., 2011; Chimin et al., 2014; Karatsoreos et al., 2010). Since we observed an expansion of WAT and BAT in response to flattening of corticosterone oscillations, we wanted to test if these liver and blood parameters were also affected.

To test if flattening of corticosterone oscillations leads to fat deposition in the liver, we performed a histological analysis of the livers of sham and corticosterone pellet-implanted mice. We did not detect fat deposition in the liver upon flattening of corticosterone oscillations (**Figure 4A**), and the organ weight of the liver remained unchanged over the treatment period of 21 days (**Figure 4B**). Also increasing the peak amplitude in the evening phase by injection of corticosterone with the same amount the corticosterone pellet releases per day did not lead to fat deposition in the liver (**Figure 4A/C**). Furthermore, no significant gene expression alterations were detected for a number of genes involved in lipid deposition upon flattening corticosterone oscillations or increasing the peak amplitude.

The analyzed genes include the fatty acid transporter *Cd36*, *Hsd11b1*, *Pepck*, *Angptl4*, and the lipolytic genes *Lipe* (Hsl) and *Pnpla2* (Atgl) (**Figure 4-figure supplement 1**). A trend towards increased gene expression was observed for *Fasn*, *Dgat2*, *Srebp1c*, and *Glut4* in corticosterone pellet-implanted and corticosterone-injected mice. As these changes in gene expression are observed as a consequence of both corticosterone treatments, they seem to be caused by the total amount of corticosterone given to both mouse models per day and were not exclusively caused by flattening of corticosterone levels (**Figure 4-figure supplement 1**).

Next, we assessed if flattening of corticosterone oscillations increases triglycerides circulating in the blood. We determined the levels of total triglycerides as well as glycerol and free fatty acids (FFA), which are the building blocks of triglycerides, in blood serum. We did not detect a difference between mice implanted with sham and corticosterone pellets (**Figure 4D-F**). Although we detected a minor significant difference in glycerol, FFA, and triglycerides between sham and corticosterone pellet-implanted mice at day 14, this effect seems unlikely to be relevant, because levels of glycerol, FFA, and triglycerides in corticosterone pellet-implanted mice did not increase over time. At the same time sham pellet-implanted control mice showed decreased glycerol, FFA, and triglyceride levels, which resulted in the described effect and can be explained due to variation between sham pellet-implanted mice. No increase in triglyceride, glycerol, and FFA levels was detected when the peak amplitude of corticosterone was increased in the evening phase (**Figure 4G-I**).

To assess the effect of flattening of corticosterone oscillations on glucose metabolism, we performed glucose tolerance tests (GTT) and insulin tolerance tests (ITT). Initially mice implanted with corticosterone pellets seemed to be more insulin-sensitive because the GTT tests showed a quicker drop in their blood plasma glucose levels after an intraperitoneal injection of glucose (**Figure 5A**). In contrast, results from the ITT pointed to corticosterone pellet-implanted mice being insulin-resistant because their blood plasma glucose levels lowered slower after an intraperitoneal injection of insulin (**Figure 5B**). Measurement of insulin concentrations in blood plasma during the GTT revealed that the corticosterone pellet-implanted mice had 3-fold higher insulin levels compared to sham pellet-

implanted mice (**Figure 5A**). The hyperinsulinemia explained how the mice with flattened corticosterone levels could remain glucose tolerant, thus resolving the discrepancy between the GTT and ITT results. In contrast, mice injected with the same dose of corticosterone that was released by the pellet per day did not reveal any differences in glucose tolerance compared to sham injected mice and did not display higher insulin levels in the blood plasma (**Figure 5C/D**), demonstrating that the flattening of the diurnal corticosterone pattern is responsible for the increased insulin levels.

To determine when insulin levels increase, we performed a time course analysis in which we monitored insulin levels in blood plasma over 21 days in the corticosterone and sham pellet-implanted mice. We found that insulin levels are more than 7-fold increased already at day 3 after flattening of corticosterone oscillations. This initial increase slowly decreased during the 21-day time course, but was still 3-fold higher at day 21 compared to control mice (**Figure 5E**). High insulin levels resulted in reduced blood glucose levels under non-fasted conditions (**Figure 5F**). Interestingly, flattening of corticosterone oscillations induced hyperinsulinemia already before expansion of the white fat depots, suggesting the high insulin might even contribute to their expansion. A summary of all parameters measured in mice upon different treatments can be found in **Figure 1-table supplement 1**.

Flattening of corticosterone oscillations results in gene expression alterations of genes involved in glycolysis, lipid metabolism and circadian rhythm.

To elucidate how gene expression is globally affected by flattening of glucocorticoid oscillations as a potential cause for the expansion of fat depots, we performed RNAseq analysis of vWAT. We chose to analyze vWAT since its expansion has been recognized to be detrimental to metabolic health, while accumulation of sWAT may be protective (Jeffery et al., 2016). Mice were subcutaneously implanted with corticosterone pellets to flatten their corticosterone oscillations, and the vWAT was harvested 0, 3, 7, and 14 days after pellet implantation. These time points were chosen based on the timepoints when expansion of BAT or WAT had been observed for the first time (**Figure 1E, 1G, and 3B**). Notably, nearly all of the differently expressed genes in vWAT at 14 days already

displayed alterations in gene expression in the same direction at 3 days after flattening corticosterone oscillations, before expansion of WAT was detected. **Figure 6A** shows that the observed alterations in gene expression cluster by the type of treatment and not by the time since pellet implantation, suggesting that cells start on an increasing transcriptional trajectory to increase vWAT mass. Since the expression profiles were shifted in the same direction, we increased the statistical power of our analysis by disregarding the length of treatment in the subsequent analysis and combining the data of vWAT isolated from mice treated with either corticosterone or sham pellet from 3-14 days. Significant differential expression was determined by an FDR corrected p-value (qval) less than 0.05. Using these cutoff criteria, we found 6233 transcripts that were differentially expressed in vWAT in mice treated with corticosterone versus sham implanted pellets (**Figure 6-table supplements 1 and 2**). 3498 of these transcripts were upregulated, and 2735 transcripts were downregulated.

To test whether these changes in gene expression were due to flattening of diurnal corticosterone oscillations and not caused by the amount of corticosterone released by the corticosterone pellet, we carried out RNAseq analysis in which we compared corticosterone and sham injected mice. As mentioned before, these mice were injected with the same amount of corticosterone released by the corticosterone pellet per day in one single injection, thereby increasing the peak amplitude of corticosterone in the evening phase. In this comparison, no alterations in gene expression were identified based on the above-mentioned cutoff criteria. In line with this finding, no clustering of the data was observed based on differently expressed genes between the different treatment groups or length of treatment (**Figure 6-figure supplement 1**). In conclusion, a high increase in the peak amplitude of corticosterone in the evening phase did not affect gene expression in vWAT. Furthermore, no differently expressed genes were observed when comparing vWAT of sham pellet-implanted mice and sham injected mice, demonstrating that the pellet implantation itself does not alter gene expression (**Figure 6-figure supplement 1**).

To obtain a global picture of pathways and gene classes affected in our transcriptomic data comparing vWAT of sham and corticosterone pellet-implanted mice, we performed gene ontology

(GO) analysis. Interestingly, we identified numerous GO terms related to glucose and lipid metabolism, which caught our attention keeping in mind the strong expansion of the white fat depots (**Figure 6-figure supplement 2; Figure 6-table supplement 3**). Amongst others, GO terms related to glucose metabolism were “glucose metabolic process”, “glucose 6-phosphate metabolic process” and “glycolytic process”. And GO terms related to lipid metabolism were “lipid localization”, “fatty acid metabolic process”, or “fatty acid transport”. Most of the GO terms associated with glucose or lipid metabolism exhibited a positive z score pointing to most genes in the corresponding category being upregulated. Indeed, we found glycolytic genes, including the rate limiting enzymes *Pfkl* and *Pkm*, and genes promoting glycolysis upregulated. (**Figure 6B/C**). Upregulation of the glycolytic genes could result in increased production of pyruvate, which would be further converted to Acetyl-CoA by the pyruvate dehydrogenase complex. Components and activators of the pyruvate dehydrogenase complex were upregulated as well, including *Pdha1*, *Dlat*, and *Pdk4*. Upregulation of these glycolytic genes possibly promotes the conversion of carbohydrates into fatty acids and might significantly contribute to lipid accumulation in the vWAT upon flattening of corticosterone oscillations.

Glucocorticoids have been shown to simultaneously increase pathways of triglyceride (TG) synthesis and breakdown (Lee et al., 2014; Peckett et al., 2011). Interestingly, flattening of daily corticosterone oscillations in mice could result in a similar situation. GO analysis pointed to numerous metabolic genes as being upregulated since most metabolic GO terms are characterized by a positive z score (**Figure 6-figure supplement 2; Figure 6-table supplement 3**). A closer inspection of specific genes categorized in these GO terms showed that flattening of corticosterone oscillations induces expression of genes involved in de novo lipogenesis, including the key enzymes fatty acid synthase (*Fasn*) and Acetyl-CoA carboxylase (*Acaca*), and genes involved in lipolysis, including the rate limiting enzyme *Pnpla2* (*Atgl*) (Haemmerle et al., 2006) (**Figure 6D/E**). In addition, we observed upregulation of several other genes important for TG synthesis and degradation, e.g. *Scd1*, *Scd2*, *Lpgat1*, *Acsl1, Acat2, Acadm, Abhd5,* and genes important for fatty acid transport like *Cd36* and *Slc27a4* (**Figure**

6D/E). Flattening of corticosterone oscillations alters expression levels of these genes and possibly tips the balance of TG synthesis and breakdown towards fat accumulation.

In addition, core components of the circadian clock and regulators of the circadian rhythm were also altered. These include *Clock*, *Arntl/Bmal1*, and *Per3* (**Figure 6F/G; Figure 6-table supplement 3**). The circadian clock are known to coordinate the timing and activity of enzymes involved in TG synthesis and breakdown (Lekkas and Paschos, 2019). For example, the circadian clock is found to control *Atgl* and *Scd1* (Paschos et al., 2013; Shostak et al., 2013). Possibly flattening of glucocorticoid oscillations affects the circadian clock, which then impacts lipid metabolism.

Flattened corticosterone oscillations in BAT induces a set of shared gene expression changes as in vWAT

To determine whether flattening of corticosterone oscillations affects gene expression globally in BAT and whether the same processes could be responsible for lipid accumulation in both BAT and vWAT, we performed RNAseq analysis of BAT. As was done for the transcriptomic analysis of vWAT, mice were subcutaneously implanted with corticosterone pellets to flatten their corticosterone oscillations and BAT was harvested 0, 3, 7, and 14 days after pellet implantation. Like in vWAT (**Figure 6A**), most differently expressed genes cluster by the type of treatment and not by the length of pellet implantation, with most gene expression alterations already apparent on day 3 (**Figure 7A**). We therefore again disregarded the length of treatment for subsequent analysis like we had done in the analysis of vWAT. As we observed with the vWAT (**Figure 6-figure supplement 1**), no clustering of the data was observed based on differently expressed genes between the different treatment groups or length of treatment (**Figure 7-figure supplement 1**), supporting that a high increase in the peak amplitude of corticosterone in the evening phase did not affect gene expression also in the BAT. Furthermore, no differently expressed genes were observed comparing BAT of sham pellet-implanted mice and sham injected mice, showing that the pellet implantation itself does not alter gene expression (**Figure 7-figure supplement 1**). In total we found 7146 transcripts differentially expressed comparing

BAT of corticosterone and sham pellet-implanted mice using the same cutoff criteria as described earlier for the analysis of vWAT. Applying these cutoff criteria, 3568 transcripts were upregulated, and 3578 transcripts were downregulated (**Figure 7-table supplements 1 and 2**).

We hypothesized that similar gene expression alterations as we had found in vWAT might also be responsible for the lipid accumulation observed in BAT and vWAT. To identify common features between vWAT and BAT, we identified common genes up- and downregulated in both tissues induced by flattening of corticosterone oscillations. In total, we identified 1370 transcripts being upregulated (**Figure 8A, Figure 8-table supplement 1**) and 995 transcripts being downregulated in vWAT and BAT (**Figure 8B, Figure 8-table supplement 1**). Among the upregulated transcripts, we did not find glycolytic enzymes indicating that most of the glycolytic enzymes were only affected by flattening of corticosterone oscillations in vWAT and not in BAT. In general, gene expression levels of the majority of genes positively correlated between vWAT and BAT (**Figure 8C**), indicating that most alterations observed in BAT can also be observed in vWAT. This underlines the hypothesis that similar gene expression alterations might be responsible for lipid accumulation in BAT as identified in vWAT. The positively correlated genes shared between BAT and vWAT when GC oscillations are lost were shown by GO terms analysis to be associated with lipid metabolism such as “regulation of lipid localization” and “lipid transport” changed in both BAT and vWAT (**Figure 8D**), suggesting that similar changes in lipid metabolism may cause the observed lipid accumulation in BAT and vWAT.

Markedly, we found that numerous genes involved in TG synthesis and degradation, as well as their regulators, were differently expressed in BAT and vWAT (**Figure 8E**). These genes include *Acaca, Pnpla2 (Atgl), Scd1, Fasn, leptin,* and *Hsd11ß1*, as well as the fatty acid transporter *Cd36* that was strongly upregulated in both tissues. Like in vWAT, GO-term analysis of BAT also pointed to alterations in lipid metabolism since many genes were found in the GO-term category “lipid storage” or “fatty acid metabolic process” (**Figure 7-figure supplement 2**). In conclusion, flattening corticosterone oscillations in BAT alters expression levels of genes involved in lipid metabolism,

including an increase in Cd36 expression that may mediate lipid uptake, thereby promoting lipid accumulation both in BAT and vWAT.

CD36ko mice are partially protected against weight gain induced by flattening of corticosterone oscillations

Since upregulation of Cd36 upon flattening of corticosterone oscillations is a common feature between WAT and BAT (**Figure 6D/8C**), we focused on the role of Cd36 since it mediates long-chain fatty acid uptake and has a role in lipid signaling, playing an important role in lipid metabolism (Pepino et al., 2014). To elucidate if Cd36 contributes to lipid accumulation in WAT and BAT, we first confirmed that Cd36 is indeed upregulated. RT-qPCR confirmed 3-fold higher mRNA levels in vWAT and 1.5-fold higher mRNA levels in BAT upon flattening of corticosterone oscillations (**Figure 9A**). To investigate the role of Cd36 in lipid accumulation upon flattening of corticosterone oscillations in vivo, we implanted sham and corticosterone pellets in Cd36ko mice and monitored their body weight for 21 days. After 21 days, corticosterone pellet-implanted Cd36ko mice weighed 6.9% more than sham implanted Cd36ko mice, which is 2.2% less than observed in wild-type mice (**Figure 9B**). In wild-type mice, corticosterone pellet-implanted mice weighed 9.1% more than sham implanted mice (**Figure 1B/9B**). In conclusion, Cd36ko mice are partially protected against body weight gain induced by flattening of corticosterone oscillations. Of note, during the experiment Cd36ko mice gained less weight compared to wild-type mice (3.2% less comparing sham pellet-implanted mice and 5.4% less comparing corticosterone pellet-implanted mice). Furthermore, corticosterone pellet-implanted Cd36ko mice started to gain weight 2 days later than corticosterone pellet-implanted wild-type mice.

To determine if the lower body weight gain of corticosterone pellet-implanted Cd36ko mice is manifested in lower organ weights of the white fat depots, sWAT and vWAT were dissected and weighed. Strikingly, vWAT of corticosterone pellet-implanted Cd36ko mice increased weight on average by only 208mg, which is 4-fold less than vWAT of wild-type mice (801mg) (**Figure 1G/9C**). Histological analysis of vWAT corroborated the protective effect of Cd36 against expansion of vWAT

(**Figure 9D**). Epididymal adipocytes of corticosterone pellet-implanted Cd36ko mice displayed lower increase in cell volume than corticosterone pellet-implanted wild-type mice (**Figure 9E**). Surprisingly, no significant difference was observed in the organ weight of sWAT between corticosterone pellet-implanted Cd36ko and wild-type mice (**Figure 9F**). In addition, no difference in cell volume of the adipocytes was observed (**Figure 9G/H**).

A protective role of a loss of Cd36 against lipid accumulation induced by flattening of corticosterone oscillations was also observed in BAT. As observed for vWAT, BAT of corticosterone pellet-implanted Cd36ko mice expanded less compared to corticosterone pellet-implanted wild-type mice (**Figure 9I**). This was substantiated by histological analysis of BAT showing less lipid accumulation and lower cell volume of brown adipocytes in Cd36ko mice compared to wild-type mice upon flattening of corticosterone oscillations (**Figure 9J/K**). Although a protective role for Cd36 loss against body weight gain and expansion of vWAT and BAT upon flattening corticosterone oscillations was detected, loss of Cd36 did not protect against hyperinsulinemia. Insulin levels even increased in corticosterone pellet-implanted Cd36ko mice compared to corticosterone pellet=implanted wild-type mice (**Figure 9-figure supplement 1**). In line and as observed in wild-type mice, corticosterone pellet implantation in Cd36ko mice resulted in lower blood glucose levels (**Figure 9-figure supplement 1**). Interestingly, higher insulin levels were also observed in sham pellet-implanted Cd36ko mice comparing them to sham pellet-implanted wild-type mice, suggesting that Cd36ko mice show in general higher insulin levels (**Figure 9-figure supplement 1**). In conclusion, loss of Cd36 artially protects vWAT and BAT from lipid accumulation induced by flattening of corticosterone oscillations. This protective effect is not observed for sWAT, pointing to depot-specific differences between the visceral and subcutaneous fat depots.

DISCUSSION

In this study we investigated explicitly the consequences of flattening GC oscillations, which occurs during chronic stress and is associated with depression, fatigue, cardiovascular disease, and

mortality of cancer patients (Adam, 2017; Doane et al., 2013; Kumari et al., 2009; Matthews et al., 2006; Sephton et al., 2013). Previously we had shown that flattening of circadian GC oscillations in mice, while keeping the overall GC concentrations the same during the day, results in body weight gain and expansion of the white fat depots (Bahrami-Nejad et al., 2018). In this study we now provide a time course analysis of these processes and show for the first time that flattening of corticosterone oscillations in mice induces expansion of the brown fat depots, as well as hyperinsulinemia. These pathologies were not observed when the GC peak amplitude was increased in the evening phase by injection of corticosterone, showing that as long as GC increases are restricted to the normal peak time period, they do not cause hyperinsulinemia or lipid accumulation in WAT and BAT. Flattening of GCs, as done in this study, results in elevation in trough concentrations and is accompanied by a reduction in peak concentrations with no change in the daily mean values. Such loss of trough or "off periods" has been previously shown to increase body weight and expansion of the white fat depots (Bahrami-Nejad et al., 2018; Dallman et al., 2000). We show in the current study that it also causes hyperinsulinemia, as well as an expansion of BAT.

GCs exhibit pleiotropic effects on lipid metabolism, simultaneously promoting lipolysis and lipid synthesis as well as increasing adipogenesis (for review, see Lee et al., 2014, 2018; Peckett et al., 2011). In this study, we aimed to elucidate gene expression changes that are directly dependent on flattened diurnal GC oscillations while keeping the normal daily mean values of GCs. In this regard our study is different from other studies carried out at high pharmacological GC concentrations because we just flattened GC levels without increasing the average normal GC concentrations. To identify genes induced by flattening of GCs, we performed RNAseq analysis of vWAT and BAT. Surprisingly, we observed similar expression changes as has been described for application of GCs at much higher concentrations (Yu et al., 2010), showing that chronic stress conditions could cause effects similar to side effects during GC medication. In vWAT we found that genes involved in TG synthesis (e.g. *Fasn, Acaca, Scd1, Scd2*), fatty acid uptake (e.g. *Cd36*), and TG degradation (e.g. *Pnpla2/Atgl*) are affected. Interestingly, functional GR binding sites have been identified for *Acaca,*

Fasn, Scd1, Scd2, and *Cd36* (Yu et al., 2010), identifying these as direct GC targets. The observed alterations in gene expression indicate that flattened GC oscillations promote lipogenesis and lipolysis at the same time, resulting in a futile cycle of TG synthesis and breakdown. This futile cycle has been described as the cause of lipid accumulation in white fat depots when GCs are applied at high concentrations (Lee et al., 2014) and is likely responsible for fat accumulation upon flattening of GC oscillations as well.

As a therapeutic treatment for obesity and related disorders, expansion of BAT, or boosting its respiratory activity with the goal to increase energy expenditure, has gained significant attention (Bartelt et al., 2011; Feldmann et al., 2009; Saito, 2013). However, how BAT is controlled by the pattern of circadian GC oscillations has not been equally investigated and could impact therapeutic strategy. Lipid accumulation in BAT upon GC treatment has been reported previously (Ketzer et al., 2019; Luijten et al., 2019; Shen et al., 2017; Strack et al., 1995), but here we show for the first time that flattening of daily corticosterone oscillations in mice leads to lipid accumulation in BAT as well. We hypothesized that this could impact the functionality of the tissue.

Our study suggests that a main consequence of flattening of GC oscillations dysregulates lipid metabolism, resulting in a futile cycle of TG synthesis and breakdown to finally cause lipid storage as has been described previously (Lee et al., 2014). This would be a similar situation as described for WAT and is supported by gene expression alterations observed for Acaca, Pnpla2 (Atgl), Scd1, Cd36, leptin, Hsd11ß1, and additional metabolic enzymes in both fat depots. Such a role of a futile cycle is also supported by a recent study that showed that development of glucocorticoid-induced obesity is not caused by a decreased UCP1-dependent thermogenic capacity (Luijten et al., 2019).

A common feature between lipid accumulation in BAT and vWAT induced by flattening of corticosterone oscillations is the strong upregulation of Cd36. Cd36 has been shown to facilitate fatty acid uptake into muscles and adipose tissue in rodents and humans (Abumrad et al., 1993; Glatz et al., 2010). Since several studies demonstrated that Cd36 deficiency protects against high fat diet induced obesity (Hajri et al., 2007; Koonen et al., 2010; Vroegrijk et al., 2013), we hypothesized that

knocking out Cd36 might protect against weight gain induced by flattening of GCs as well. Indeed, we found that Cd36ko mice are partially protected against body weight gain and lipid accumulation in vWAT and BAT. This can likely be explained by its role in fatty acid intake, but also additional aspects of Cd36 functionality related to fatty acid metabolism including fat taste perception, fat absorption, and fat utilization cannot be excluded (for review, see Pepino et al., 2014).

Finally, it has been reported that BAT of mice lacking Cd36 display a whitened phenotype and increased lipid droplet size (Anderson et al., 2015). However, in the current study we did not detect differences in BAT weight or lipid droplet size between sham pellet-implanted Cd36ko and wild-type mice, which might also be explained by the fact that younger mice were used in this study, which had less time to accumulate fat. Although Cd36ko did not prevent hyperinsulinemia upon flattening of corticosterone oscillations, we observed higher insulin levels in Cd36ko versus wild-type mice implanted with sham pellets. Furthermore we found a trend towards lower plasma glucose levels in Cd36ko mice, which was reported before in Cd36ko mice (Febbraio et al., 1999) and using a Cd36 inhibitor in mice (Yang et al., 2018). This suggests that metabolic actions of Cd36 are more complex and cannot be reduced to its role as a fatty acid transporter. Cd36 deficiency has been shown to affect insulin signaling (Samovski et al., 2018) and to generate intracellular PPARG ligands which activate PPARG signaling (Nagy et al., 1998; Tontonoz et al., 1998). By being highly expressed in immune cells and adipocytes, Cd36 has been implicated in the development of insulin resistance and diabetes. A soluble form of Cd36 circulating in the blood plasma has been identified as a novel marker of insulin resistance in diabetes (Alkhatatbeh et al., 2013; Handberg et al., 2010). These findings suggest Cd36 is a potential target for intervention of metabolic disorders associated with obesity.

In summary, the data presented in this study identify consequences of flattening of GCs that is frequently observed during chronic stress, underlining that small alterations or losing the normal diurnal GC oscillation pattern can result in obesity. Similar to clinical treatments with higher GC concentrations, we show that flattening of GCs has pleiotropic effects on gene expression in a multiple organ systems, including BAT and WAT. Markedly, knocking out just one component, the fatty acid

transporter Cd36, partially prevents body weight gain and lipid accumulation. We show that in addition to increasing lipid uptake, flattening of glucocorticoids promotes TG synthesis and breakdown at the same time, which together results in lipid accumulation in BAT and WAT. Finally, our transcriptomic data of different BAT and WAT depots further supports the close link between stress biology and energy metabolism, a crosstalk that is more widely recognized as stress/metabolism comorbidities emerge as complicating factors in metabolic disease and psychiatric disorders, including depression.

REFERENCES

Abumrad NA, El-Maghrabi MR, Amri EZ, Lopez E, Grimaldi PA. 1993. Cloning of a rat adipocyte membrane protein implicated in binding or transport of long-chain fatty acids that is induced during preadipocyte differentiation. Homology with human CD36. *J Biol Chem* **268**:17665–17668.

Adam EK. 2017. Diurnal Cortisol Slopes and Mental and Physical Health Outcomes:A Systematic Review and Meta-analysis. *Psychoneuroendcrinology* **Sep**:25–41. doi:110.1016/j.bbi.2017.04.008

Alkhatatbeh MJ, Enjeti AK, Acharya S, Thorne RF, Lincz LF. 2013. The origin of circulating CD36 in type 2 diabetes. *Nutr Diabetes* **3**:e59-7. doi:10.1038/nutd.2013.1

Anderson CM, Kazantzis M, Wang J, Venkatraman S, Goncalves RLS, Quinlan CL, Ng R, Jastroch M, Benjamin DI, Nie B, Herber C, Van AAN, Park MJ, Yun D, Chan K, Yu A, Vuong P, Febbraio M, Nomura DK, Napoli JL, Brand MD, Stahl A. 2015. Dependence of brown adipose tissue function on CD36-mediated coenzyme Q uptake. *Cell Rep* **10**:505–515. doi:10.1016/j.celrep.2014.12.048

Andrews S, Babraham Bioinformatics. 2010. FastQC: A quality control tool for high throughput sequence data. *Manual*. doi:citeulike-article-id:11583827

Bahrami-Nejad Z, Zhao ML, Tholen S, Hunerdosse D, Tkach KE, van Schie S, Chung M, Teruel MN. 2018. A Transcriptional Circuit Filters Oscillating Circadian Hormonal Inputs to Regulate Fat Cell Differentiation. *Cell Metab* **27**:854-868.e8. doi:10.1016/j.cmet.2018.03.012

Bartelt A, Bruns OT, Reimer R, Hohenberg H, Ittrich H, Peldschus K, Kaul MG, Tromsdorf UI, Weller H, Waurisch C, Eychmüller A, Gordts PLSM, Rinninger F, Bruegelmann K, Freund B, Nielsen P, Merkel M, Heeren J. 2011. Brown adipose tissue activity controls triglyceride clearance. *Nat Med* **17**:200–206. doi:10.1038/nm.2297

Betz MJ, Enerbäck S. 2015. Human brown adipose tissue: What we have learned so far. *Diabetes* **64**:2352–2360. doi:10.2337/db15-0146

Bowles NP, Karatsoreos IN, Li X, Vemuri VK, Wood J-A, Li Z, Tamashiro KLK, Schwartz GJ, Makriyannis AM, Kunos G, Hillard CJ, McEwen BS, Hill MN. 2015. A peripheral endocannabinoid mechanism contributes to glucocorticoid-mediated metabolic syndrome. *Proc Natl Acad Sci* **112**:285–290. doi:10.1073/pnas.1421420112

Bray NL, Pimentel H, Melsted P, Pachter L. 2016. Near-optimal probabilistic RNA-seq quantification. *Nat Biotechnol* **34**:525–527. doi:10.1038/nbt.3519

Broussard JL, Cauter E Van. 2016. Disturbances of sleep and circadian rhythms: Novel risk factors for obesity. *Curr Opin Endocrinol Diabetes Obes*. doi:10.1097/MED.0000000000000276

Campbell JE, Peckett AJ, D'Souza AM, Hawke TJ, Riddell MC. 2011. Adipogenic and lipolytic effects of chronic glucocorticoid exposure. *Am J Physiol - Cell Physiol* **300**:C198-209. doi:10.1152/ajpcell.00045.2010

Cannon B, Nedergaard J. 2004. Brown Adipose Tissue: Function and Physiological Significance. *Physiol Rev* **84**:277–359. doi:10.1152/physrev.00015.2003

Chimin P, Farias TDSM, Torres-Leal FL, Bolsoni-Lopes A, Campaña AB, Andreotti S, Lima FB. 2014. Chronic glucocorticoid treatment enhances lipogenic activity in visceral adipocytes of male Wistar rats. *Acta Physiol* **211**:409–420. doi:10.1111/apha.12226

Chusyd DE, Wang D, Huffman DM, Nagy TR. 2016. Relationships between Rodent White Adipose Fat Pads and Human White Adipose Fat Depots. *Front Nutr* **3**. doi:10.3389/fnut.2016.00010

Cypess AM, Lehman S, Williams G, Tal I, Rodman D, Goldfine AB, Kuo FC, Palmer EL, Tseng YH, Doria A, Kolodny GM, Ronald Kahn C. 2009. Identification and importance of brown adipose tissue in adult humans. *Obstet Gynecol Surv* **64**:519–520. doi:10.1097/OGX.0b013e3181ac8aa2

Dallman MF, Akana SF, Bhatnagar S, Bell ME, Strack AM. 2000. Bottomed out: Metabolic significance of the circadian trough in glucocorticoid concentrations. *Int J Obes* **24**:S40–S46. doi:10.1038/sj.ijo.0801276

Doane LD, Mineka S, Zinbarg RE, Craske M, Griffith JW, Adam EK. 2013. Are flatter diurnal cortisol rhythms associated with major depression and anxiety disorders in late adolescence? the role of life stress and daily negative emotion. *Dev Psychopathol* **25**:629–642. doi:10.1017/S0954579413000060

Febbraio M, Abumrad NA, Hajjar DP, Sharma K, Cheng W, Pearce SFA, Silverstein RL. 1999. A null mutation in murine CD36 reveals an important role in fatty acid and lipoprotein metabolism. *J Biol Chem* **274**:19055–19062. doi:10.1074/jbc.274.27.19055

Feldmann HM, Golozoubova V, Cannon B, Nedergaard J. 2009. UCP1 Ablation Induces Obesity and Abolishes Diet-Induced Thermogenesis in Mice Exempt from Thermal Stress by Living at Thermoneutrality. *Cell Metab* **9**:203–209. doi:10.1016/j.cmet.2008.12.014

Galarraga M, Campión J, Muñoz-Barrutia A, Boqué N, Moreno H, Martínez JA, Milagro F, Ortiz-de-Solórzano C. 2012. Adiposoft: automated software for the analysis of white adipose tissue cellularity in histological sections. *J Lipid Res* **53**:2791–2796. doi:10.1194/jlr.D023788

Glatz JFC, Luiken JJFP, Bonen A. 2010. Membrane fatty acid transporters as regulators of lipid metabolism: Implications for metabolic disease. *Physiol Rev* **90**:367–417. doi:10.1152/physrev.00003.2009

Haemmerle G, Lass A, Zimmermann R, Gorkiewicz G, Meyer C, Rozman J, Heldmaier G, Maier R, Theussl C, Eder S, Kratky D, Wagner EF, Klingenspor M, Hoefler G, Zechner R. 2006. Defective lipolysis and altered energy metabolism in mice lacking adipose triglyceride lipase. *Science* **211**:734–738.

Hajri T, Hall AM, Jensen DR, Pietka TA, Drover VA, Tao H, Eckel R, Abumrad NA. 2007. CD36-facilitated fatty acid uptake inhibits leptin production and signaling in adipose tissue. *Diabetes* **56**:1872–1880. doi:10.2337/db06-1699

Handberg A, Norberg M, Stenlund H, Hallmans G, Attermann J, Eriksson JW. 2010. Soluble CD36 (sCD36) clusters with markers of insulin resistance, and high sCD36 is associated with increased type 2 diabetes risk. *J Clin Endocrinol Metab* **95**:1939–1946. doi:10.1210/jc.2009-2002

Harms M, Seale P. 2013. Brown and beige fat: Development, function and therapeutic potential. *Nat Med* **19**:1252–1263. doi:10.1038/nm.3361

Hodes GE, Brookshire BR, Hill-Smith TE, Teegarden SL, Berton O, Lucki I. 2012. Strain differences in the effects of chronic corticosterone exposure in the hippocampus. *Neuroscience* **222**:269–280. doi:10.1016/j.neuroscience.2012.06.017

Jeffery E, Wing A, Holtrup B, Sebo Z, Kaplan JL, Saavedra-Peña R, Church CD, Colman L, Berry R, Rodeheffer MS. 2016. The Adipose Tissue Microenvironment Regulates Depot-Specific Adipogenesis in Obesity. *Cell Metab* **24**:142–150. doi:10.1016/j.cmet.2016.05.012

Karatsoreos IN, Bhagat SM, Bowles NP, Weil ZM, Pfaff DW, McEwen BS. 2010. Endocrine and physiological changes in response to chronic corticosterone: A potential model of the metabolic syndrome in mouse. *Endocrinology* **151**:2117–2127. doi:10.1210/en.2009-1436

Ketzer LA, Mousovich-Neto F, de Melo Reis RA, Atella GC, Carvalho DP, Costa ACR, Corrêa da Costa VM, Matos MS, Miranda-Alves L. 2019. Brown adipose tissue remodeling induced by corticosterone in Wistar male rats. *Exp Physiol* 1–15. doi:10.1113/ep087332

Koonen DPY, Sung MMY, Kao CKC, Dolinsky VW, Koves TR, Ilkayeva O, Jacobs RL, Vance DE, Light PE, Muoio DM, Febbraio M, Dyck JRB. 2010. Alterations in skeletal muscle fatty acid handling predisposes middle-aged mice to diet-induced insulin resistance. *Diabetes* **59**:1366–1375. doi:10.2337/db09-1142

Kumari M, Badrick E, Chandola T, Adam EK, Stafford M, Marmot MG, Kirschbaum C, Kivimaki M. 2009. Cortisol secretion and fatigue: Associations in a community based cohort. *Psychoneuroendocrinology* **34**:1476–1485. doi:10.1016/j.psyneuen.2009.05.001

Kusminski CM, Bickel PE, Scherer PE. 2016. Targeting adipose tissue in the treatment of obesity-associated diabetes. *Nat Rev Drug Discov* **15**:639–660. doi:10.1038/nrd.2016.75

Lee MJ, Pramyothin P, Karastergiou K, Fried SK. 2014. Deconstructing the roles of glucocorticoids in adipose tissue biology and the development of central obesity. *Biochim Biophys Acta* **1842**:473–481. doi:10.1016/j.bbadis.2013.05.029

Lee RA, Harris CA, Wang J-C. 2018. Glucocorticoid Receptor and Adipocyte Biology. *Nucl Recept Res* **5**:1–21. doi:10.32527/2018/101373

Lekkas D, Paschos GK. 2019. Autonomic Neuroscience : Basic and Clinical The circadian clock control of adipose tissue physiology and metabolism. *Auton Neurosci Basic Clin* **219**:66–70. doi:10.1016/j.autneu.2019.05.001

Lightman S, Terry JR. 2014. The importance of dynamic signalling for endocrine regulation and drug development: Relevance for glucocorticoid hormones. *Lancet Diabetes Endocrinol* **2**:593–599. doi:10.1016/S2213-8587(13)70182-7

Luijten IHN, Brooks K, Boulet N, Shabalina IG, Jaiprakash A, Carlsson B, Fischer AW, Cannon B, Nedergaard J. 2019. Glucocorticoid-Induced Obesity Develops Independently of UCP1. *Cell Rep* **27**:1686-1698.e5. doi:10.1016/j.celrep.2019.04.041

Matthews K, Schwartz J, Cohen S, Seeman T. 2006. Diurnal cortisol decline is related to coronary calcification: CARDIA study. *Psychosom Med* **68**:657–661. doi:10.1097/01.psy.0000244071.42939.0e

Miller GE, Chen E, Zhou ES. 2007. If it goes up, must it come down? Chronic stress and the hypothalamic-pituitary-adrenocortical axis in humans. *Psychol Bull* **133**:25–45. doi:10.1037/0033-2909.133.1.25

Nagy L, Tontonoz P, Alvarez JGA, Chen H, Evans RM. 1998. Oxidized LDL regulates macrophage gene expression through ligand activation of PPARγ. *Cell* **93**:229–240. doi:10.1016/S0092-8674(00)81574-3

Oster H, Damerow S, Kiessling S, Jakubcakova V, Abraham D, Tian J, Hoffmann MW, Eichele G. 2006. The circadian rhythm of glucocorticoids is regulated by a gating mechanism residing in the adrenal cortical clock. *Cell Metab* **4**:163–173. doi:10.1016/j.cmet.2006.07.002

Paschos GK, Ibrahim S, Song W, Kunieda T, Reyes TM, Bradfield CA, Vaughan CH, Eiden M, Masoodi M, Griffin JL, Wang F, Lawson JA, Garret A. 2013. Obesity in mice with adipocyte-specific deletion of clock component Arntl. *Nat Med* **18**:1768–1777. doi:10.1038/nm.2979.Obesity

Peckett AJ, Wright DC, Riddell MC. 2011. The effects of glucocorticoids on adipose tissue lipid

metabolism. *Metabolism* **60**:1500–1510. doi:10.1016/j.metabol.2011.06.012

Pepino MY, Kuda O, Samovski D, Abumrad NA. 2014. Structure-Function of CD36 and Importance of Fatty Acid Signal Transduction in Fat Metabolism. *Annu Rev Nutr* **34**:281–303. doi:10.1146/annurev-nutr-071812-161220

Pimentel H, Bray NL, Puente S, Melsted P, Pachter L. 2017. Differential analysis of RNA-seq incorporating quantification uncertainty. *Nat Methods* **14**:687–690. doi:10.1038/nmeth.4324

Rebuffé-Scrive M, Walsh UA, McEwen B, Rodin J. 1992. Effect of chronic stress and exogenous glucocorticoids on regional fat distribution and metabolism. *Physiol Behav* **52**:583–590. doi:10.1016/0031-9384(92)90351-2

Saito M. 2013. Brown adipose tissue as a regulator of energy expenditure and body fat in humans. *Diabetes Metab J* **37**:22–29. doi:10.4093/dmj.2013.37.1.22

Saito M, Okamatsu-Ogura Y, Matsushita M, Watanabe K, Yoneshiro T, Nio-Kobayashi J, Iwanaga T, Miyagawa M, Kameya T, Nakada K, Kawai Y, Tsujisaki M. 2009. High incidence of metabolically active brown adipose tissue in healthy adult humans: Effects of cold exposure and adiposity. *Diabetes* **58**:1526–1531. doi:10.2337/db09-0530

Samovski D, Dhule P, Pietka T, Jacome-Sosa M, Penrose E, Son NH, Flynn CR, Shoghi KI, Hyrc KL, Goldberg IJ, Gamazon ER, Abumrad NA. 2018. Regulation of insulin receptor pathway and glucose metabolism by CD36 signaling. *Diabetes* **67**:1272–1284. doi:10.2337/db17-1226

Sephton SE, Lush E, Dedert EA, Floyd AR, Rebholz WN, Dhabhar FS, Spiegel D, Salmon P. 2013. Diurnal cortisol rhythm as a predictor of lung cancer survival. *Brain Behav Immun* **30**. doi:10.1016/j.bbi.2012.07.019

Shen Y, Roh HC, Kumari M, Rosen ED. 2017. Adipocyte glucocorticoid receptor is important in lipolysis and insulin resistance due to exogenous steroids, but not insulin resistance caused by high fat feeding. *Mol Metab* **6**:1150–1160. doi:10.1016/j.molmet.2017.06.013

Shostak A, Meyer-Kovac J, Oster H. 2013. Circadian regulation of lipid mobilization in white adipose tissues. *Diabetes* **62**:2195–2203. doi:10.2337/db12-1449

Sidossis L, Kajimura S. 2015. Brown and beige fat in humans: Thermogenic adipocytes that control energy and glucose homeostasis. *J Clin Invest* **125**:478–486. doi:10.1172/JCI78362

Strack AM, Bradbury MJ, Dallman MF. 1995. Corticosterone decreases nonshivering thermogenesis and increases lipid storage in brown adipose tissue. *Am J Physiol - Regul Integr Comp Physiol* **268**:R183–R191. doi:10.1152/ajpregu.1995.268.1.r183

Tontonoz P, Nagy L, Alvarez JGA, Thomazy VA, Evans RM. 1998. PPARγ promotes monocyte/macrophage differentiation and uptake of oxidized LDL. *Cell* **93**:241–252. doi:10.1016/S0092-8674(00)81575-5

Van Marken Lichtenbelt WD, Vanhommerig JW, Smulders NM, Drossaerts JMAFL, Kemerink GJ, Bouvy ND, Schrauwen P, Teule GJJ. 2009. Cold-activated brown adipose tissue in healthy men. *N Engl J Med* **360**:1500–1508. doi:10.1056/NEJMoa0808718

Vroegrijk IOCM, Van Klinken JB, Van Diepen JA, Van Den Berg SAA, Febbraio M, Steinbusch LKM, Glatz JFC, Havekes LM, Voshol PJ, Rensen PCN, Van Dijk KW, Van Harmelen V. 2013. CD36 is important for adipocyte recruitment and affects lipolysis. *Obesity* **21**:2037–2045. doi:10.1002/oby.20354

Walter W, Sánchez-Cabo F, Ricote M. 2015. GOplot: An R package for visually combining expression data with functional analysis. *Bioinformatics*. doi:10.1093/bioinformatics/btv300

Weitzman ED, Fukushima D, Nogeire C, Roffwarg H, Gallagher TF, Hellman L. 1971. Twenty-four hour pattern of the episodic secretion of cortisol in normal subjects. *J Clin Endocrinol Metab* **33**:14–22. doi:10.1210/jcem-33-1-14

Yang J, Park KW, Cho S. 2018. Inhibition of the CD36 receptor reduces visceral fat accumulation and improves insulin resistance in obese mice carrying the BDNF-Val66Met variant. *J Biol Chem* **293**:13338–13348. doi:10.1074/jbc.RA118.002405

Yu CY, Mayba O, Lee J V., Tran J, Harris C, Speed TP, Wang JC. 2010. Genome-wide analysis of glucocorticoid receptor binding regions in adipocytes reveal gene network involved in triglyceride homeostasis. *PLoS One* **5**. doi:10.1371/journal.pone.0015188

Yu G, Wang LG, Han Y, He QY. 2012. ClusterProfiler: An R package for comparing biological themes among gene clusters. *Omi A J Integr Biol*. doi:10.1089/omi.2011.0118

AUTHOR CONTRIBUTIONS

S.T. and M.N.T. conceived the project. S.T. performed and analyzed all experiments with assistance of A.R., E.B.M., and W.Y. K.K. analyzed transcriptomic data. S.T. and M.N.T wrote the paper with input from all authors.

ACKNOWLEDGEMENTS

This work was supported by National Institutes of Health RO1-DK101743, RO1-DK106241, P50-GM107615, and Stanford BioX Seed Grant funding (to M.N.T.). Furthermore we acknowledge the funding from the Deutsche Forschungsgemeinschaft (DFG) TH 2156/1-1 (to S.T.), the Stanford Bio-X Program and Novo Nordisk Foundation NNF16OC0018642 (to A.R.), and American Heart Association Postdoctoral Fellowship 18POST34030448 (to E.B.M.). We thank Prof. Fredric B. Kraemer and all members of the Teruel Lab for discussions and critical reading of the manuscript. We also thank the Stanford Animal Histology Services (AHS) for paraffin embedding of fat tissue and performing H&E staining.

FIGURE LEGENDS

Figure 1: Time course analysis of lipid accumulation in WAT induced by flattening of circadian corticosterone oscillations. (A) Time course of average corticosterone levels in mice implanted with corticosterone pellets compared to mice implanted with sham pellets 7 days after pellet implantation. n = 3 for sham pellet; n = 4 for corticosterone pellet, mean ± SEM. (B) Time course showing body weight gain of mice implanted with corticosterone pellets compared to mice implanted with sham pellets. n = 11, mean ± SEM. Unpaired t test (sham pellet versus cort pellet), *$p < 0.05$, **$p < 0.01$, ***$p < 0.001$, ****$p < 0.0001$. (C) Average daily food intake of each mouse per cage (n = 8). Up to 5 mice were housed in each cage. Food intake was monitored for 14 days, mean ± SD. Unpaired t-test, ns = not significant. (D, F) Images of sWAT and vWAT after pellet implantation for 21 days. (E, G) Weight of sWAT and vWAT at different time points after pellet implantation, n = 5-9, mean ± SD. Unpaired t test, **$p < 0.01$, ****$p < 0.0001$. (H, J) Images of sWAT and vWAT stained with hematoxylin and eosin at 3, 7, 14, and 21 days after pellet implantation. One representative staining is shown for each timepoint (n = 3). Scale bars 50μm. (I, K) Frequency distributions of mean lipid droplet area in sWAT and vWAT as analyzed using Adiposoft (mean + SEM; n=3 mice per treatment, 25 images per mouse (20x)). See also Figure 1-table supplement 1.

Figure 2: Increasing the peak amplitude of corticosterone in the evening phase does not affect body weight gain or lipid accumulation in WAT. (A) Time course of average corticosterone levels in mice injected with corticosterone compared to mice injected with solvent control 7 days after start of injections. n = 3-4, mean ± SEM. (B) Time course showing body weight gain of mice injected with corticosterone compared to mice injected with solvent control. n = 9, mean ± SEM. (C) Average daily food intake of each mouse per cage (n = 7). Up to 5 mice were housed in each cage. Food intake was monitored for 14 days, mean ± SD. Unpaired t test, **$p < 0.01$, ns = not significant. (D, G) Images of sWAT and vWAT from sham and corticosterone injected mice 21 days after start of daily injections. (E, H) Weight of sWAT at different time points after start of daily injections, n = 3-8, mean ± SD. (F, I) Time course of sWAT after start of injections. WAT was stained with hematoxylin and eosin at 3, 7, 14, and 21 days after start of treatment. One representative staining is shown (n = 3). Scale bars 50μm.

Figure 3: Flattening of daily corticosterone oscillations in mice results in lipid accumulation in BAT. (A) Interscapular BAT of sham and corticosterone pellet-implanted mice 14 days after start of treatment. (B) Weight of interscapular BAT at different time points after pellet implantation, n = 5-9, mean ± SD. Unpaired t test, **$p < 0.01$, ****$p < 0.0001$. (C) Time course of BAT after pellet implantation. BAT was stained with hematoxylin and eosin at 3, 7, 14, and 21 days after pellet implantation. One representative staining is shown (n = 3-7). Scale bars 50μm. (D) Frequency distribution of mean lipid droplet area in BAT as analyzed using Adiposoft (mean + SEM; for day 3, 7, 14 n = 3; for day 21 n = 5 mice per treatment, 25 images per mouse (20x)). (E) BAT of sham and corticosterone injected mice 14 days after start of treatment. (F) Weight of BAT at different time points after start of daily injections, n = 3-8, mean ± SD. (G) Time course of BAT after start of injection. BAT was stained with hematoxylin and eosin at 3, 7, 14, and 21 days after start of injection. One representative staining is shown (n = 3-7). Scale bars 50 μm.

Figure 4: Flattening of corticosterone oscillations does not elevate circulating triglycerides in blood or result in fat deposition in the liver. (A) H&E staining of livers 21 days after pellet implantation / start of injection. One representative staining is shown (n = 4). **(B)** Weight of livers at different time points after pellet implantation, n = 4-5, mean ± SD. **(C)** Weight of livers at different time points after start of daily injections, n = 3-4, mean ± SD. **(D-I)** Time courses of changes in FFA, glycerol, and triglycerides measured in blood serum over 14 days. n = 4-5 for pellet-implanted mice, n = 3-4 for

injected mice, mean ± SEM, unpaired t test, *p < 0.05, ns = not significant. See also Figure 4-figure supplement 1.

Figure 5: Flattening of corticosterone oscillations causes hyperinsulinemia. (A) Glucose tolerance test (GTT) of sham and corticosterone pellet-implanted mice after 21 days of treatment; mean ± SEM; n = 5; unpaired t test, *p < 0.05, ***p < 0.001, ****p < 0.0001. **(B)** Insulin tolerance test (ITT) of sham and corticosterone pellet-implanted mice after 17 days of treatment; mean ± SEM; n = 5 for sham pellet; n = 6 for corticosterone pellet; unpaired t test, *p < 0.05, **p < 0.01. **(C)** Glucose tolerance test (GTT) of sham and corticosterone injected mice after 21 days of treatment; mean ± SEM; n = 6. **(D)** Insulin tolerance test (ITT) of sham and corticosterone injected mice after 17 days of treatment; mean ± SEM; n = 5 for sham injection; n = 6 for corticosterone injection. **(E)** Time course of insulin levels in blood plasma in sham and corticosterone pellet-implanted mice (not fasted); mean +/- SEM; n = 6; unpaired t test, *p < 0.05, **p < 0.01, ****p < 0.0001. **(F)** Blood glucose levels in sham and corticosterone pellet-implanted mice (not fasted) 14 days after pellet implantation; mean +/- SEM; n = 9; unpaired t test, **p < 0.01.

Figure 6: Flattening of corticosterone oscillations results in gene expression alterations in vWAT of genes involved in glycolysis, lipid metabolism and circadian rhythms. (A) Principal component analysis of vWAT samples obtained at 3, 7, and 14 days after implantation of corticosterone or sham pellets in mice. **(B-G)** Comparison of the vWAT transcriptomes of corticosterone and sham pellet-implanted mice. **(B-C)** Glycolytic genes are highlighted in green. **(D-E)** Selected genes relevant for lipid metabolism are highlighted in green, orange, purple, and pink. **(F-G)** Selected genes involved in circadian rhythm are highlighted in green. See also Figure 6-figure supplements 1 and 2 and Figure 6-table supplements 1-3.

Figure 7: Flattened corticosterone oscillations in BAT result in altered gene expression of thermogenic genes as well as genes involved in oxidative phosphorylation. (A) Principal component analysis of vWAT samples obtained at 3, 7, and 14 days after implantation of corticosterone or sham pellets in mice. **(B-C)** Comparison of the BAT transcriptomes of corticosterone and sham pellet-implanted mice. **(B-C)** Genes related to thermogenesis and oxidative phophorylation are highlighted in green and orange, respectively. See also Figure 7-figure supplements 1 and 2 and Figure 7-table supplements 1 and 2.

Figure 8: Transcriptomic analysis of BAT and vWAT upon flattening of corticosterone oscillations reveals similar gene expression alterations of genes involved in lipid turnover. (A/B) Venn diagram showing overlap of genes differently expressed in BAT and vWAT upon flattening of corticosterone oscillations. **(C)** Correlation of log2 fold changes between the vWAT and BAT transcriptomes upon flattening of corticosterone oscillations. **(D)** GO terms positively correlated in WAT and BAT. GO terms related to lipid metabolism are highlighted. **(E)** Log 2 fold changes of selected genes involved in lipid metabolism and circadian rhythms comparing vWAT and BAT upon flattening of corticosterone oscillations. See also Figure 8-table supplement 1.

Figure 9: Cd36ko partially protects against fat gain due to flattening of corticosterone oscillations. (A) mRNA expression for Cd36 measured by qPCR in vWAT and BAT of sham and corticosterone pellet-implanted mice 3 and 14 days after implantation. Gene expression data was normalized to the expression of Tbp and is presented as mean ± SEM (n = 3-4). Unpaired t test, *p < 0.05, **p < 0.01, ***p < 0.001, ns = not significant. Control group are mice at start of experiment (day 0). **(B)** Time course showing body weight gain of wild type and Cd36ko mice implanted with corticosterone pellets compared to mice implanted with sham pellets. n = 10-12, mean ± SEM. Unpaired t test (red asterisk: WT + sham pellet versus Cd36ko + sham pellet; blue asterisk: WT + corticosterone pellet versus Cd36ko + corticosterone pellet; black asterisk: sham versus

corticosterone pellet), *$p < 0.05$, **$p < 0.01$, ***$p < 0.001$, ****$p < 0.0001$. **(C)** Weight of epididymal (visceral) fat depots 21 days after pellet implantation, n = 5-12, mean ± SD. Unpaired t test, *$p < 0.05$, ****$p < 0.0001$. **(D)** H&E staining of vWAT 21 days after pellet implantation. One representative staining is shown (n = 3-5). Scale bars 50μm. **(E)** Frequency distribution of mean adipocyte area in vWAT as analyzed using Adiposoft (mean + SEM; n=3-5, 25 images per mouse (20x)). **(F)** Weight of inguinal (subcutaneous) fat depots 21 days after pellet implantation, n = 5-12, mean ± SD. Unpaired t test, ****$p < 0.0001$. **(G)** H&E staining of sWAT 21 days after pellet implantation. One representative staining is shown (n = 4-5). Scale bars 50μm. **(H)** Frequency distribution of mean adipocyte area in sWAT as analyzed using Adiposoft (mean + SEM; n=4-5, 25 images per mouse (20x)). **(I)** Weight of BAT 21 days after pellet implantation, n = 5-12, mean ± SD. Unpaired t test, *$p < 0.05$, ***$p < 0.001$, ****$p < 0.0001$. **(J)** H&E staining of BAT 21 days after pellet implantation. One representative staining is shown (n = 4-5). Scale bars 50μm. **(K)** Frequency distribution of mean adipocyte area in BAT as analyzed using Adiposoft (mean + SEM; n=4-5, 25 images per mouse (20x)). See also Figure 9-figure supplement 1.

SUPPLEMENTARY FIGURES

Figure 4-figure supplement 1: Flattening of corticosterone oscillations does not result in significant gene expression alterations of genes involved in lipid metabolism in liver. (A-J) Gene expression of different genes measured by qPCR in liver after flattening corticosterone levels for 14 days. Gene expression data was normalized to the expression of Tbp and is presented as mean ± SEM (n = 3-4). Unpaired t test, *p < 0.05, **p < 0.01, ns = not significant. Control group are mice at beginning of experiment (day 0).

Figure 6-figure supplement 1: Transcriptomic analysis of vWAT. (A) Principal component analysis of vWAT samples of corticosterone and sham injected mice 3, 7, and 14 days after start of injections. **(B)** Number of significantly changed transcripts in the different comparisons of treatment methods.

Figure 6-figure supplement 2: GO analysis comparing the transcriptome of vWAT from sham and corticosterone pellet-implanted mice. GO terms in the categories **(A)** Biological Process and **(B)** Cellular Component were categorized based on common topics. GO term analysis was done using the clusterProfiler package (Yu et al., 2012). GO terms of interest were identified by calculating the adjusted p-value comparing corticosterone pellet vs. sham pellet as well as a z score for general trends of increased or decreased differential expression of the genes within the GO terms. The z score is defined as the number of genes within the GO term with an absolute value log2 fold change greater than or equal to 1.5 (fold change > 1.5 or < 0.67) divided by the square root of the total number of genes assigned to that GO term.

Figure 7-figure supplement 1: Transcriptomic analysis of BAT. (A) Principal component analysis of BAT samples of corticosterone and sham injected mice 3, 7, and 14 days after start of injections. **(B)** Number of significantly changed transcripts in the different comparisons of treatment methods.

Figure 7-figure supplement 2: GO analysis comparing the transcriptome of BAT from sham and corticosterone pellet-implanted mice. GO terms in the categories Biological Process and Cellular Component were categorized based on common topics. GO term analysis was done using the clusterProfiler package (Yu et al., 2012). GO terms of interest were identified by calculating the adjusted p-value comparing corticosterone pellet vs. sham pellet as well as a z score for general trends of increased or decreased differential expression of the genes within the GO terms. The z score is defined as the number of genes within the GO term with an absolute value log2 fold change greater than or equal to 1.5 (fold change > 1.5 or < 0.67) divided by the square root of the total number of genes assigned to that GO term.

Figure 9-figure supplement 1: Cd36ko mice are not protected against hyperinsulinemia caused by flattening of corticosterone. (A) Insulin levels in blood plasma in sham and corticosterone pellet-implanted Cd36ko and wild-type mice (not fasted) 14 days after pellet implantation; mean +/- SEM; n = 5-7; unpaired t test, *p < 0.05, **p < 0.01. **(B)** Blood glucose levels in sham and corticosterone pellet-implanted Cd36ko and wild-type mice (not fasted) 14 days after pellet implantation; mean +/- SEM; n = 6-9; unpaired t test, **p < 0.01.

SUPPLEMENTARY TABLES

Figure 1-table supplement 1: Summary of mouse experiments. All data was acquired after a treatment period of 21 days, except data for blood glucose (not fasted), FFA, glycerol, and triglyceride levels, which were determined 14 days after beginning of treatment. Values are presented as mean +/- SEM; n.d. = no data.

Figure 6-table supplement 1: Transcript levels of differentially expressed genes comparing vWAT of corticosterone and sham pellet-implanted mice.

Figure 6-table supplement 2: Gene expression levels of differentially expressed genes comparing vWAT of corticosterone and sham pellet-implanted mice.

Figure 6-table supplement 3: Gene ontology (GO) analysis of RNAseq data comparing vWAT of corticosterone and sham pellet-implanted mice.

Figure 7-table supplement 1: Transcript levels of differentially expressed genes comparing BAT of corticosterone and sham pellet-implanted mice.

Figure 7-table supplement 2: Gene expression levels of differentially expressed genes comparing BAT of corticosterone and sham pellet-implanted mice.

Figure 8-table supplement 1: Differentially expressed genes identified in RNAseq analysis of vWAT and BAT comparing corticosterone and sham pellet-implanted mice.

METHODS

Mice

Mice were housed in small groups of five or fewer on a 12h light/dark cycle (lights on at 7:00 hours) with food and water access ad libitum in the animal facility at Stanford University. All mice were maintained on a normal chow diet and only male mice were used for experiments. All animal care and experimentation was conducted in accordance with current NIH and Stanford University Institutional Animal Care and Use Committee guidelines. Seven-week-old C57BL/6J male mice were purchased from Jackson Laboratory (cat. 000664) and housed in the animal facility for 7 days prior the start of experiments. Cd36ko mice were published before (Febbraio et al., 1999). Cd36ko breeding pairs were purchased from Jackson Laboratory (cat. 019006). For the experiments 8-week old male mice were used. All mice were dissected between 13:00 and 18:00 alternating corticosterone-treated and control mice. A summary of all parameters measured in mice upon different treatments can be found in **Figure 1-table supplement 1**.

Corticosterone administration in mice

To flatten circadian glucocorticoid oscillations, mice were implanted subcutaneously with corticosterone releasing pellets (5mg, 21-day release; Innovative Research of America, Sarasota, FL, USA). Sham pellets were implanted as control. For pellet implantation mice were anesthetized via inhalation of isoflurane, when anesthetized an incision equal in diameter to that of the pellet was made on the lateral side of the neck and the pellet inserted using a trochar. Mice weighed an average of 24.1 ± 1.2 g, which results in a daily dose of 9 mg/kg/day.

For injections corticosterone complexed with 2-hydroxypropyl-β-cyclodextrin (C174, Sigma) was dissolved in PBS and injected subcutaneously once daily at 17:00 for up to 21 days with the same corticosterone dose (9 mg/kg/day) as released by the corticosterone pellets per day.

Measurement of corticosterone in blood serum

Blood was taken at multiple time points over a 15 h time period. At the first time point blood was taken by nicking the tail vain. Blood samples collected on following time points were taken by removal of the crust formed after first blood withdrawal. The blood was allowed to clot by leaving it undisturbed at room temperature for 45 minutes. The clot was removed by centrifuging at 2000 x g for 15 minutes. The corticosterone concentration in blood serum was determined using the Enzyme Immunoassay kit (K014-H1, Arbor Assays, Michigan, USA) following the manufacturer's instructions.

Glucose Tolerance Test

Before the procedure mice were fasted for 16h in clean cages with no food or feces in the bedding. At 9am blood glucose levels were measured with a glucometer (Diathrive, South Salt Lake, Utah, USA) by obtaining a drop of blood from the tail. Subsequently, mice received 2 g of glucose (Sigma G8270) / kg of body weight by intraperitoneal injection. Blood glucose levels were measured again after 15, 30, 60, and 120 min after injection.

To measure insulin levels 20 μl of blood were collected from the tail before glucose injection and on every following time point and mixed with heparin. The blood plasma was prepared by centrifugation at 2000 x g for 15 minutes. The insulin concentration in blood plasma was determined using the Ultra Sensitive Mouse Insulin ELISA Kit (Cat. 90080, Crystal Chem, Illinois, USA) following the manufacturer's instructions.

Insulin Tolerance Test

Before the procedure mice were fasted for 6h in clean cages with no food or feces in the bedding starting at 9am. Blood glucose levels were measured with a glucometer (Diathrive, South Salt Lake, Utah, USA) by obtaining a drop of blood from the tail. Subsequently, mice were injected with 0.75 units/kg body weight of human insulin (Sigma I9278) by intraperitoneal injection. Blood glucose levels were measured again after 15, 30, 45, 60, and 120 min after injection.

To measure insulin levels 20 μl of blood were collected from the tail before glucose injection and on every following time point and mixed with heparin. The blood plasma was prepared by centrifugation at 2000 x g for 15 minutes. The insulin concentration in blood plasma was determined using the Ultra Sensitive Mouse Insulin ELISA Kit (Cat. 90080, Crystal Chem, Illinois, USA) following the manufacturer's instructions.

Measuring concentrations of FFA, glycerol, and triglycerides

FFA contents in blood serum were determined the Free Fatty Acid Quantitation Kit (Sigma, MAK044) following the manufacturers' protocols. Glycerol and triglyceride concentrations in blood serum were measured using the Triglyceride Determination Kit (Sigma, TR0100) following the manufacturer's instructions.

Histology

For histological examination interscapular brown adipose tissue (BAT), inguinal white adipose tissue (sWAT), and epididymal white adipose tissue (vWAT) were fixed in 4% formalin for 24h directly after dissection. Tissues were rinsed and stored in 95% until embedding in paraffin. Paraffin blocks were sectioned (10μm) and sections mounted on glass slides and stained with hematoxylin and eosin (H & E). Images were taken at 20x magnification and the adipocyte area was calculated using the Fiji software plug-in Adiposoft (Galarraga et al., 2012).

Reverse transcription quantitative polymerase chain reaction

Total RNA was extracted from fat tissues using the RNeasy Lipid Tissue Mini Kit (Qiagen, Hilden, Germany) and from liver using the RNeasy Mini Kit (Qiagen, Hilden, Germany). Equal amounts of RNA were reverse-transcribed to cDNA using the iScript cDNA Synthesis system (Bio-Rad, Hercules, CA, USA). Relative transcript amounts were measured by qPCR using PowerUp SYBR Green Master Mix (Appliedbiosystems, Vilnius, Lithuania). All expression data were normalized to TATA-binding

protein (Tbp) expression. The primer sequences were as follows: Cd36 forward → 5'-ATG GGC TGT GAT CGG AAC TG-3'; Cd36 reverse → 5'-TTT GCC ACG TCA TCT GGG TTT-3'; Tbp forward → 5'-GAA GCT GCG GTA CAA TTC CAG-3'; Tbp reverse → 5'-CCC CTT GTA CCC TTC ACC AAT-3'; Ucp1 forward → 5'-AGC CGG CTT AAT GAC TGG AG-3'; Ucp1 reverse → 5'-TCT GTA GGC TGC CCA ATG AAC-3'; Angptl4 forward → 5'- CAT CCT GGG ACG AGA TGA ACT -3'; Angptl4 reverse → 5'- TGA CAA GCG TTA CCA CAG GC -3'; Pepck forward → 5'- CTG CAT AAC GGT CTG GAC TTC -3'; Pepck reverse → 5'- GCC TTC CAC GAA CTT CCT CAC -3'; Lipe (Hsl) forward → 5'- GAT TTA CGC ACG ATG ACA CAG T -3'; Lipe (Hsl) reverse → 5'- ACC TGC AAA GAC ATT AGA CAG C -3'; Glut4 forward → 5'- ATC ATC CGG AAC CTG GAG G -3'; Glut4 reverse → 5'- CGG TCA GGC GCT TTA GAC TC -3'; Srebp1 forward → 5'- TGA CCC GGC TAT TCC GTG A -3'; Srebp1 reverse → 5'- CTG GGC TGA GCA ATA CAG TTC -3'; Fasn forward → 5'- GGA GGT GGT GAT AGC CGG TAT -3'; Fasn reverse → 5'- TGG GTA ATC CAT AGA GCC CAG -3'; Hsd11ß1 forward → 5'- GGA GCC CAT GTG GTA TTG ACT -3'; Hsd11ß1 reverse → 5'- CCG CAA ATG TCA TGT CTT CCA T -3'; Dgat2 forward → 5'- GCG CTA CTT CCG AGA CTA CTT -3'; Dgat2 reverse → 5'- GGG CCT TAT GCC AGG AAA CT -3'; Atgl (Pnpla2) forward → 5'- ATG TTC CCG AGG GAG ACC AA -3'; Atgl (Pnpla2) reverse → 5'- GAG GCT CCG TAG ATG TGA GTG -3'.

RNAseq

RNA was extracted from BAT or vWAT using the RNeasy Lipid Tissue Mini Kit (Qiagen, Hilden, Germany). For each condition (sham pellet, corticosterone pellet, sham injection, corticosterone injection) RNA was extracted from 4 mice per time point (3, 7, 14 days). RNA was also isolated from 4 mice before start of treatment (day 0). RNA quality of all samples was evaluated by Bioanalyzer 2100 High Sensitivity RNA Analysis chips (Agilent, Cat. 5067-1513) which displayed intact RNA integrity. mRNA samples were concentrated to ≤ 5 μl by MinElute column (QIAGEN, Cat. 74204). For generation of RNA-seq libraries, polyadenylated mRNA was isolated from 300 ng of total RNA by incubation with oligo-DT attached magnetic beads and followed by strand-specific library preparation

using the TruSeq Stranded mRNA Library Preparation kit (Ilumina, Cat. 20020595). Briefly, isolated polyadenylated mRNA was fragmented using divalent cations under elevated temperature and 1st and 2nd strands DNA were synthesized using SuperScript II Reverse Transcriptase (provided with Ilumina kit). A-tailing and adapter ligation was performed according to the manufacturer's protocol; the resulting dsDNA was enriched in a PCR reaction based on predetermined CT values and cleaned using AMPure XP beads (provided with Ilumina kit). Concentrations of enriched dsDNA fragments with specific adapters were determined and base pair average size and library integrity were analyzed using the Bioanalyzer DNA High Sensitivity chips (Agilent, Cat. 5067-4626). Samples were pooled and sequenced on the Illumina NextSeq 500/550 High Output platform (Illumina, FC-404-2002) up to 18 samples per lane with 1% PhiX spike as a control.

To assess the read quality of the raw FASTQ files we used FastQC (Andrews and Babraham Bioinformatics, 2010) (v0.11.7). Pseudo-alignment of the reads to the mouse reference transcriptome (Mus_musculus.GRCm38.cdna) was carried out using Kallisto (Bray et al., 2016) (v0.44.0) with the quantification algorithm enabled, the number of bootstraps set to 100, and ran in paired-end mode. The Kallisto output files imported to R with Sleuth, and the transcripts per million (TPM) were used for downstream differential expression analysis (Pimentel et al., 2017).

We used the Sleuth package to identify differentially expressed genes with the full model consisting of treatment, lane, replicate, and day and the reduced model consisting of lane and replicate. This allowed us to identify genes that were differentially expressed based on treatment (i.e. corticosterone pellet vs sham pellet) and time. All downstream analysis was done on transcripts that were considered significant from the DESeq2 analysis (likelihood ratio test with a FDR less than 0.05). Outlier samples were identified by both clustering and PCA analysis and removed. The number of differentially expressed genes after removing outliers increased by 1,668, with all but 31 genes common between the two models.

For more information, please see https://kylekovary.shinyapps.io/Flattened-circadian-glucocorticoid-oscillations/.

Gene Ontology (GO) Analysis

GO term analysis was done using the clusterProfiler package (Yu et al., 2012). GO terms of interest were identified by calculating the adjusted p-value between two sample groups (i.e. corticosterone pellet vs. sham pellet) as well as a z score for general trends of increased or decreased differential expression of the genes within the GO terms. The z score is defined as the number of genes within the GO term with an absolute value log2 fold change greater than or equal to 1.5 (fold change > 1.5 or < 0.67) divided by the square root of the total number of genes assigned to that GO term (Walter et al., 2015).

Western Blot Analysis

For western blot analysis 10mg of fat tissue were lysed in 50 mM Tris-HCl, 1 % Nonidet P-40, 0.1 % sodium dodecyl sulfate (SDS) and 0.15 M NaCl, pH 8, supplemented with protease inhibitors (cOmplete, Mini, EDTA-free, Sigma Aldrich). For preparation of tissue lysates, a homogenizer (Fisher Scientific) was used and cell debris removed by centrifugation at max speed for 20 min at 4 °C. Protein concentrations were determined using the bicinchoninic acid (BCA) protein assay kit (Pierce, Rockford, USA). 50 µg of proteins of tissue lysates were boiled for 5 min at 95°C in NuPAGE LDS sample buffer containing 1x reducing agent (Invitrogen). Lysates were separated by SDS–PAGE using the XCell SureLock Electrophoresis Cell on NuPAGE Novex 4%–12% Bis-Tris Protein Gels (Invitrogen). Proteins were transferred onto polyvinylidene fluoride membranes (Thermo Scientific) using the XCell II Blot Module (Invitrogen). Membranes were blocked by incubating with TBS with 0.1% Tween-20 containing 3% non-fat milk for 2h at room temperature or overnight at 4°C. After blocking, membranes were exposed to the primary antibody (UCP-1; used 1:800) overnight at 4°C. After washing (TBS with 0.1% Tween-20), the membranes were incubated for 2 h with the secondary antibody. The membranes were washed (TBS with 0.1% Tween-20) and developed with the Supersignal West Femto chemiluminescence substrate (Pierce, Rockford, USA). Peroxidase activity

was detected with a Lumi Imager device (ImageQuant LAS 4000mini, GE Healthcare). The primary antibody UCP-1 was purchased from α-Diagnostics (Catalog No. UCP11-A). The secondary antibody was purchased from Cell Signaling (α-rabbit: Catalog No. #7074).

Statistics

All data are represented as mean ± SD or mean ± SEM and analyzed by Students t test using GraphPad Prism software. n indicates the number of animals per group or number of independent experiments. Results were considered significant if $p < 0.05$.

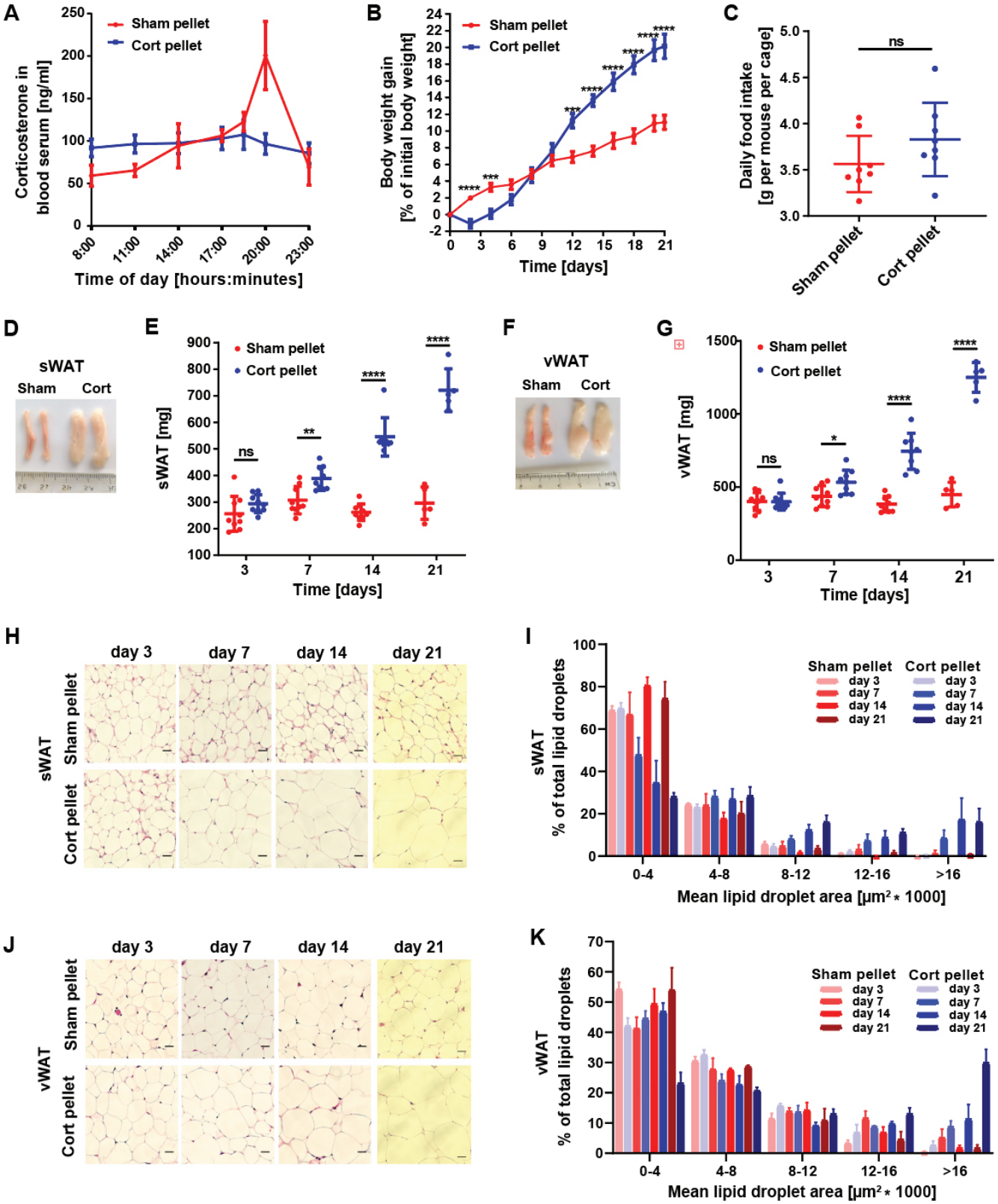

Fig. 1: Time course analysis of lipid accumulation in WAT induced by flattening of circadian corticosterone oscillations. (A) Time course of average corticosterone levels in mice implanted with corticosterone pellets compared to mice implanted with sham pellets 7 days after pellet implantation. n = 3 for sham pellet; n = 4 for corticosterone pellet, mean ± SEM. (B) Time course showing body weight gain of mice implanted with corticosterone pellets compared to mice implanted with sham pellets. n = 11, mean ± SEM. Unpaired t test (sham pellet versus cort pellet), *p < 0.05, **p < 0.01, ***p < 0.001, ****p < 0.0001. (C) Average daily food intake of each mouse per cage (n = 8). Up to 5 mice were housed in each cage. Food intake was monitored for 14 days, mean ± SD. Unpaired t test, ns = not significant. (D, F) Images of sWAT and vWAT after pellet implantation for 21 days. (E, G) Weight of sWAT and vWAT at different time points after pellet implantation, n = 5-9, mean ± SD. Unpaired t test, **p < 0.01, ****p < 0.0001. (H, J) Images of sWAT and vWAT stained with hematoxylin and eosin at 3, 7, 14, and 21 days after pellet implantation. One representative staining is shown for each timepoint (n = 3). Scale bars 50μm. (I, K) Frequency distributions of mean lipid droplet area in sWAT and vWAT as analyzed using Adiposoft (mean + SEM; n=3 mice per treatment, 25 images per mouse (20x)). See also Figure 1-table supplement 1.

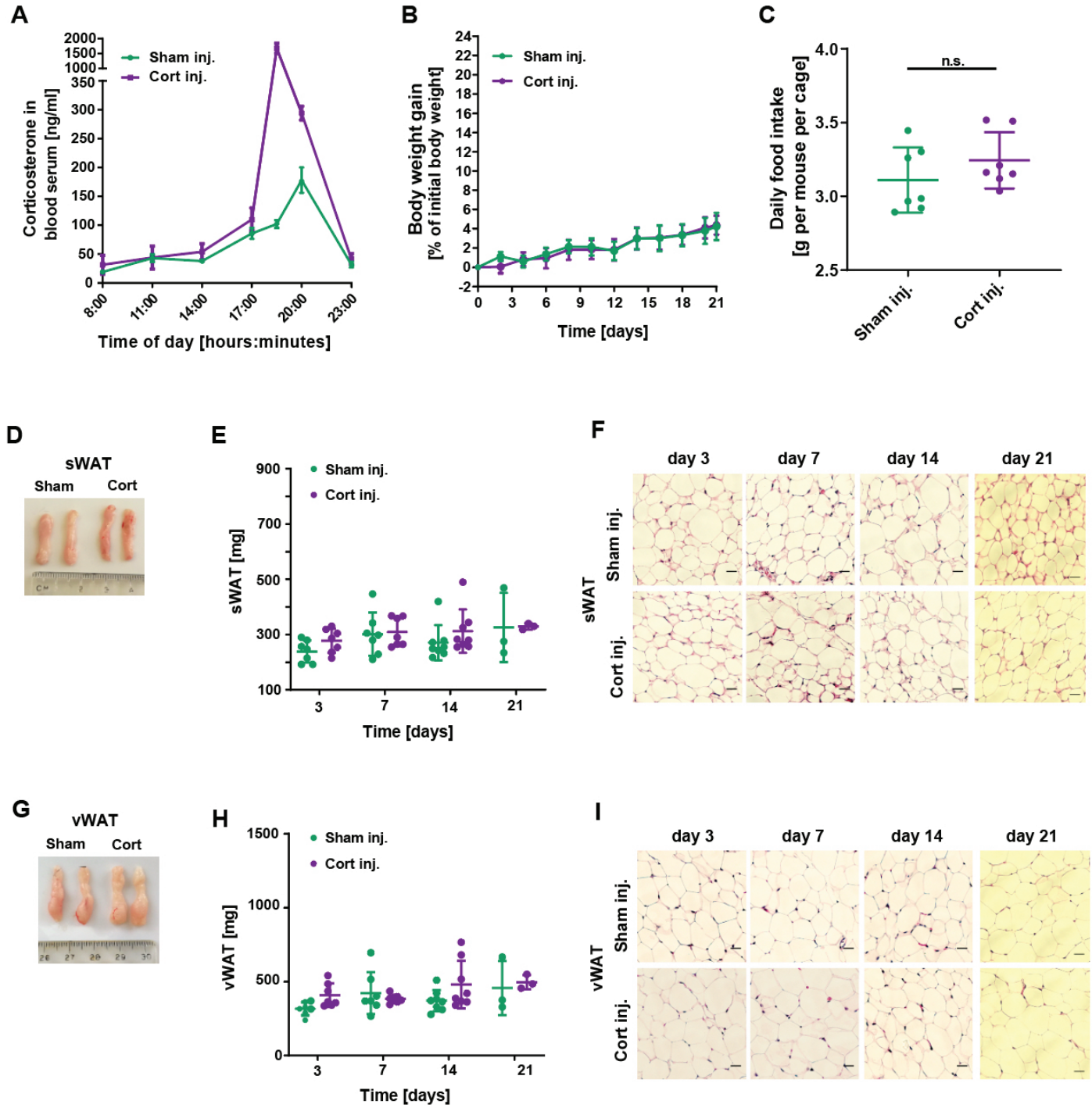

Fig. 2: Increasing the peak amplitude of corticosterone in the evening phase does not affect body weight gain or lipid accumulation in WAT. (A) Time course of average corticosterone levels in mice injected with corticosterone compared to mice injected with solvent control 7 days after start of injections. n = 3-4, mean ± SEM. (B) Time course showing body weight gain of mice injected with corticosterone compared to mice injected with solvent control. n = 9, mean ± SEM. (C) Average daily food intake of each mouse per cage (n = 7). Up to 5 mice were housed in each cage. Food intake was monitored for 14 days, mean ± SD. Unpaired t test, $^{**}p < 0.01$, ns = not significant. (D, G) Images of sWAT and vWAT from sham and corticosterone injected mice 21 days after start of daily injections. (E, H) Weight of sWAT at different time points after start of daily injections, n = 3-8, mean ± SD. (F, I) Time course of sWAT after start of injections. WAT was stained with hematoxylin and eosin at 3, 7, 14, and 21 days after start of treatment. One representative staining is shown (n = 3). Scale bars 50μm.

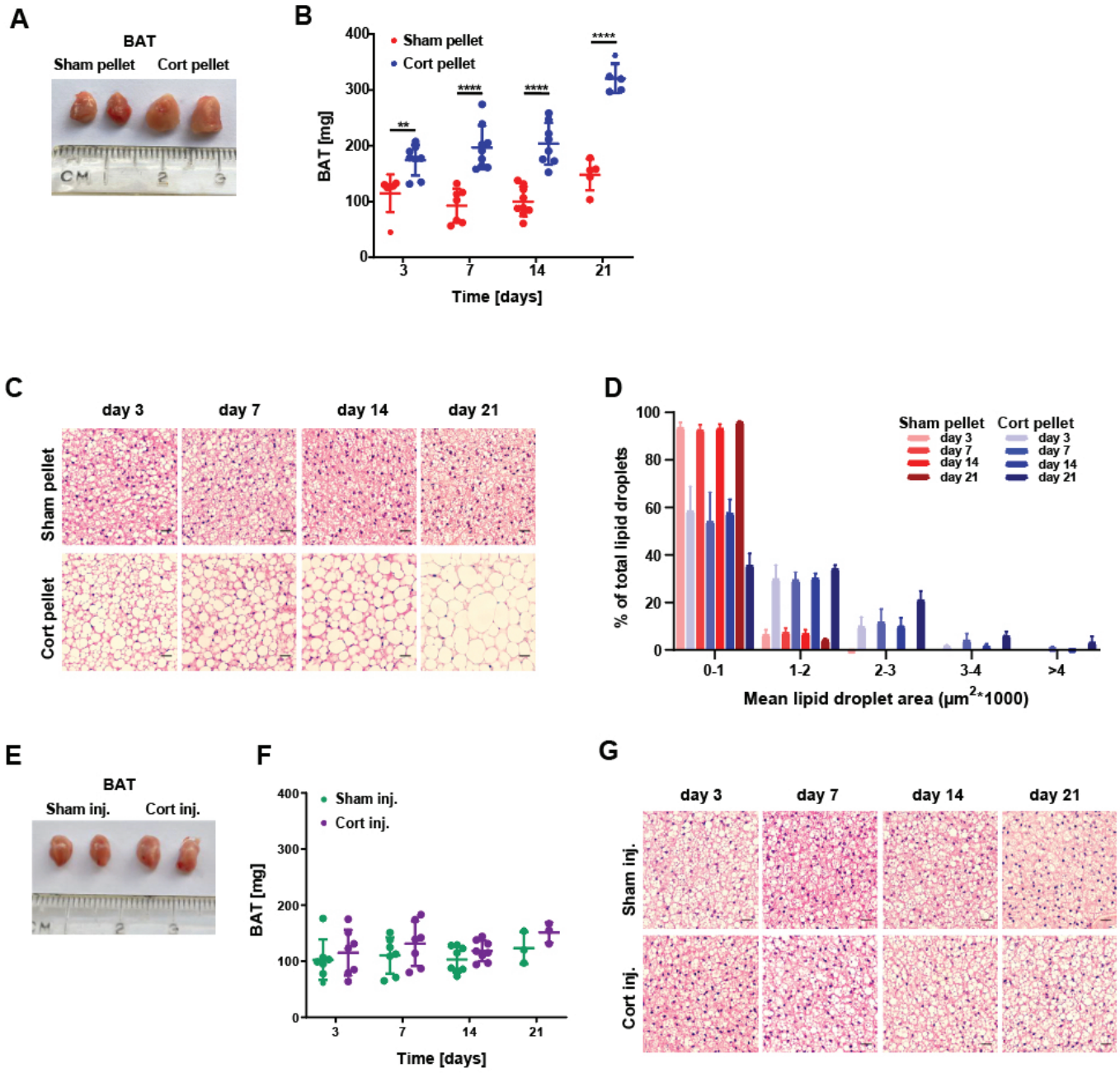

Fig. 3: Flattening of daily corticosterone oscillations in mice results in lipid accumulation in BAT. (A) Interscapular BAT of sham and corticosterone pellet implanted mice 14 days after start of treatment. (B) Weight of interscapular BAT at different time points after pellet implantation, n = 5-9, mean ± SD. Unpaired t test, $^{**}p < 0.01$, $^{****}p < 0.0001$. (C) Time course of BAT after pellet implantation. BAT was stained with hematoxylin and eosin at 3, 7, 14, and 21 days after pellet implantation. One representative staining is shown (n = 3-7). Scale bars 50μm. (D) Frequency distribution of mean lipid droplet area in BAT as analyzed using Adiposoft (mean + SEM; for day 3, 7, 14 n = 3; for day 21 n = 5 mice per treatment, 25 images per mouse (20x)). (E) BAT of sham and corticosterone injected mice 14 days after start of treatment. (F) Weight of BAT at different time points after start of daily injections, n = 3-8, mean ± SD. (G) Time course of BAT after start of injection. BAT was stained with hematoxylin and eosin at 3, 7, 14, and 21 days after start of injection. One representative staining is shown (n = 3-7). Scale bars 50 μm.

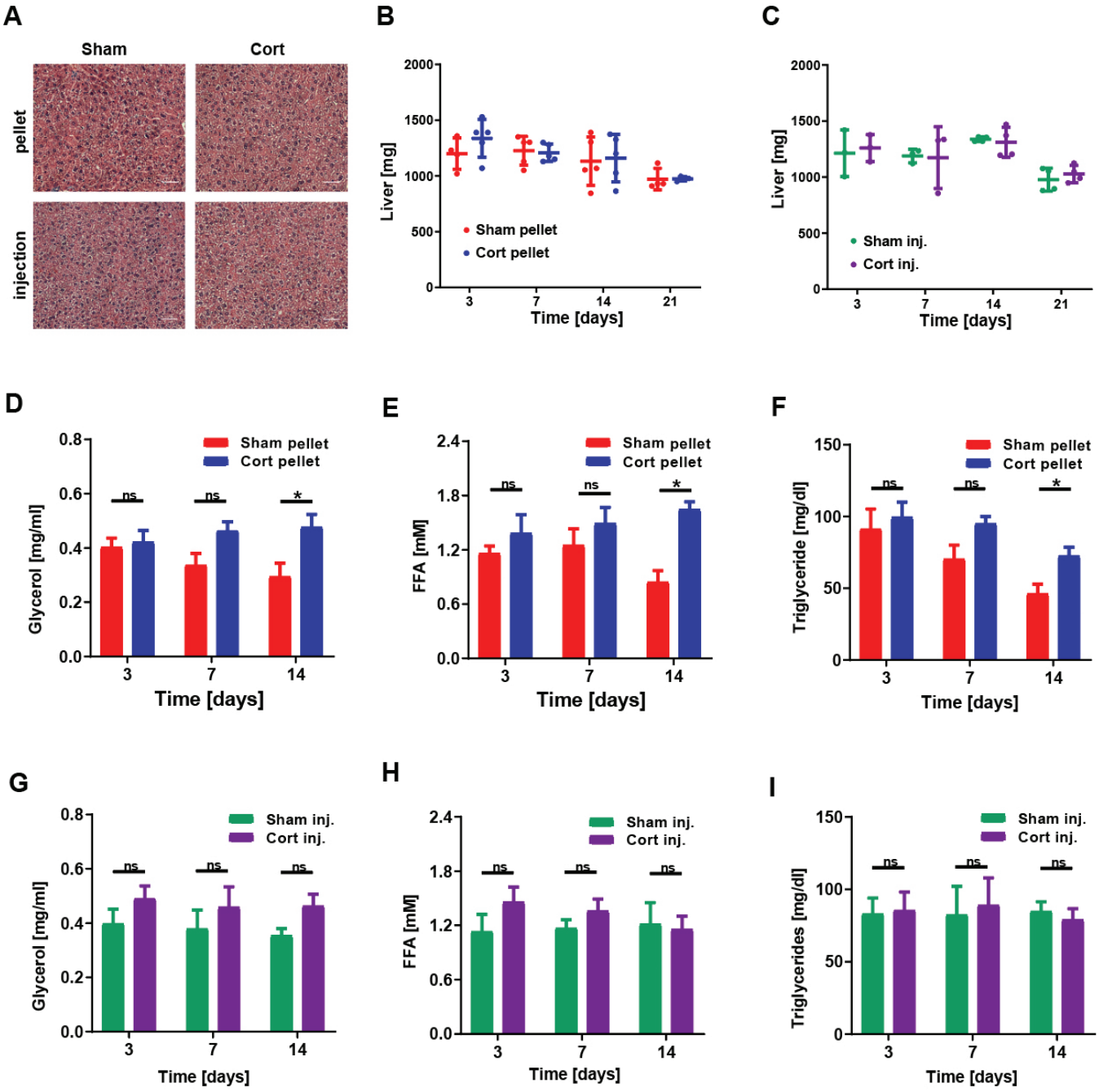

Fig. 4: Flattening of corticosterone oscillations does not result in fat deposition in the liver or elevate circulating triglycerides in blood. (A) H&E staining of livers 21 days after pellet implantation / start of injection. One representative staining is shown (n = 4). (B) Weight of livers at different time points after pellet implantation, n = 4-5, mean ± SD. (C) Weight of livers at different time points after start of daily injections, n = 3-4, mean ± SD. (D-I) Time courses of changes in FFA, glycerol, and triglycerides measured in blood serum over 14 days. n = 4-5 for pellet implanted mice, n = 3-4 for injected mice, mean ± SEM, unpaired t test, *$p < 0.05$, n.s. = not significant. See also Figure 4-figure supplement 1.

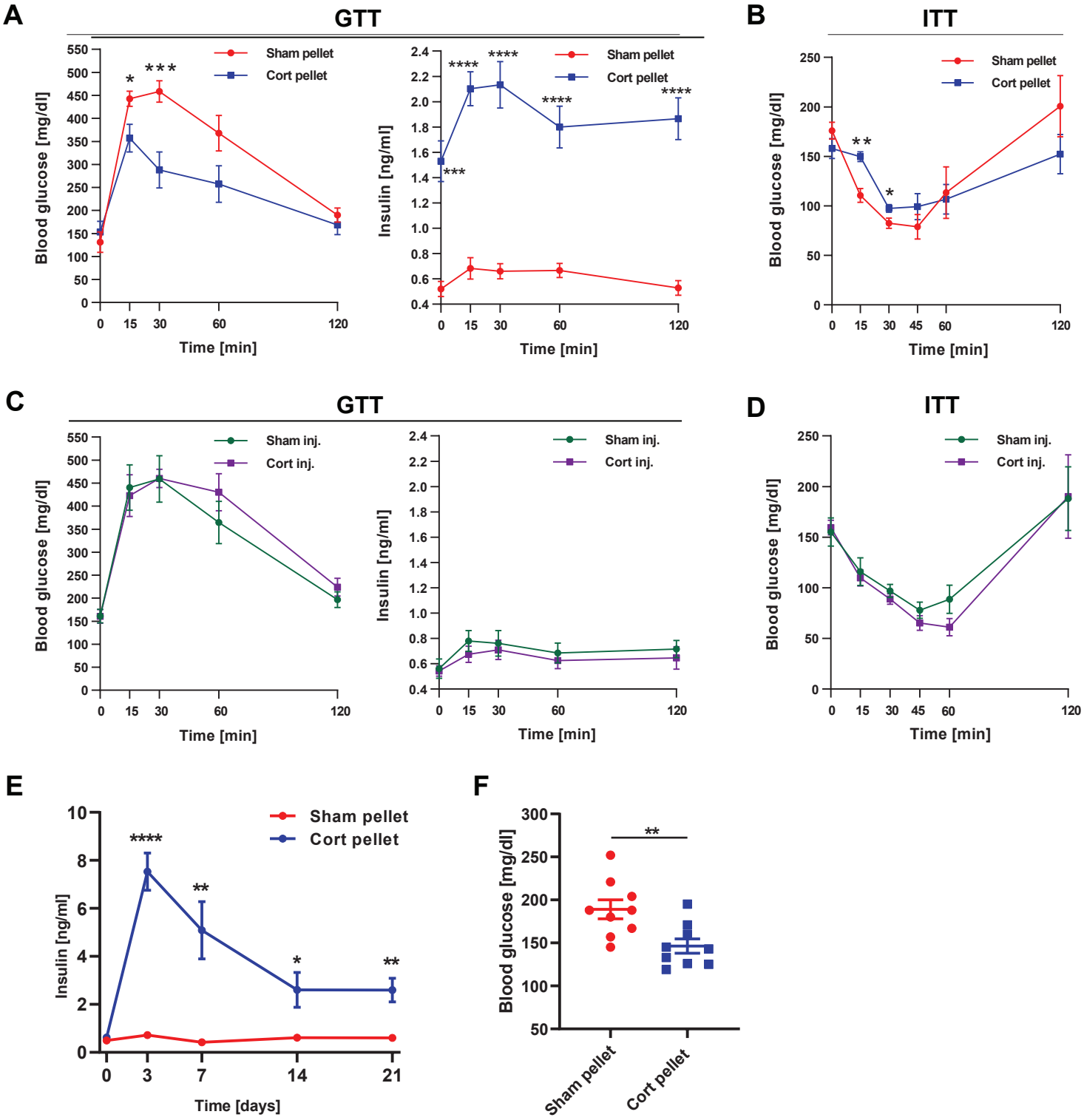

Fig. 5: Flattening of corticosterone oscillations causes hyperinsulinemia. (A) Glucose tolerance test (GTT) of sham and corticosterone pellet implanted mice after 21 days of treatment; mean ± SEM; n = 5; unpaired t test, *p < 0.05, ***p < 0.001, ****p < 0.0001. (B) Insulin tolerance test (ITT) of sham and corticosterone pellet implanted mice after 17 days of treatment; mean ± SEM; n = 5 for sham pellet; n = 6 for corticosterone pellet; unpaired t test, *p < 0.05, **p < 0.01. (C) Glucose tolerance test (GTT) of sham and corticosterone injected mice after 21 days of treatment; mean ± SEM; n = 6. (D) Insulin tolerance test (ITT) of sham and corticosterone injected mice after 17 days of treatment; mean ± SEM; n = 5 for sham injection; n = 6 for corticosterone injection. (E) Time course of insulin levels in blood plasma in sham and corticosterone pellet implanted mice (not fasted); mean +/- SEM; n = 6; unpaired t test, *p < 0.05, **p < 0.01, ****p < 0.0001. (F) Blood glucose levels in sham and corticosterone pellet implanted mice (not fasted) 14 days after pellet implantation; mean +/- SEM; n = 9; unpaired t test, **p < 0.01.

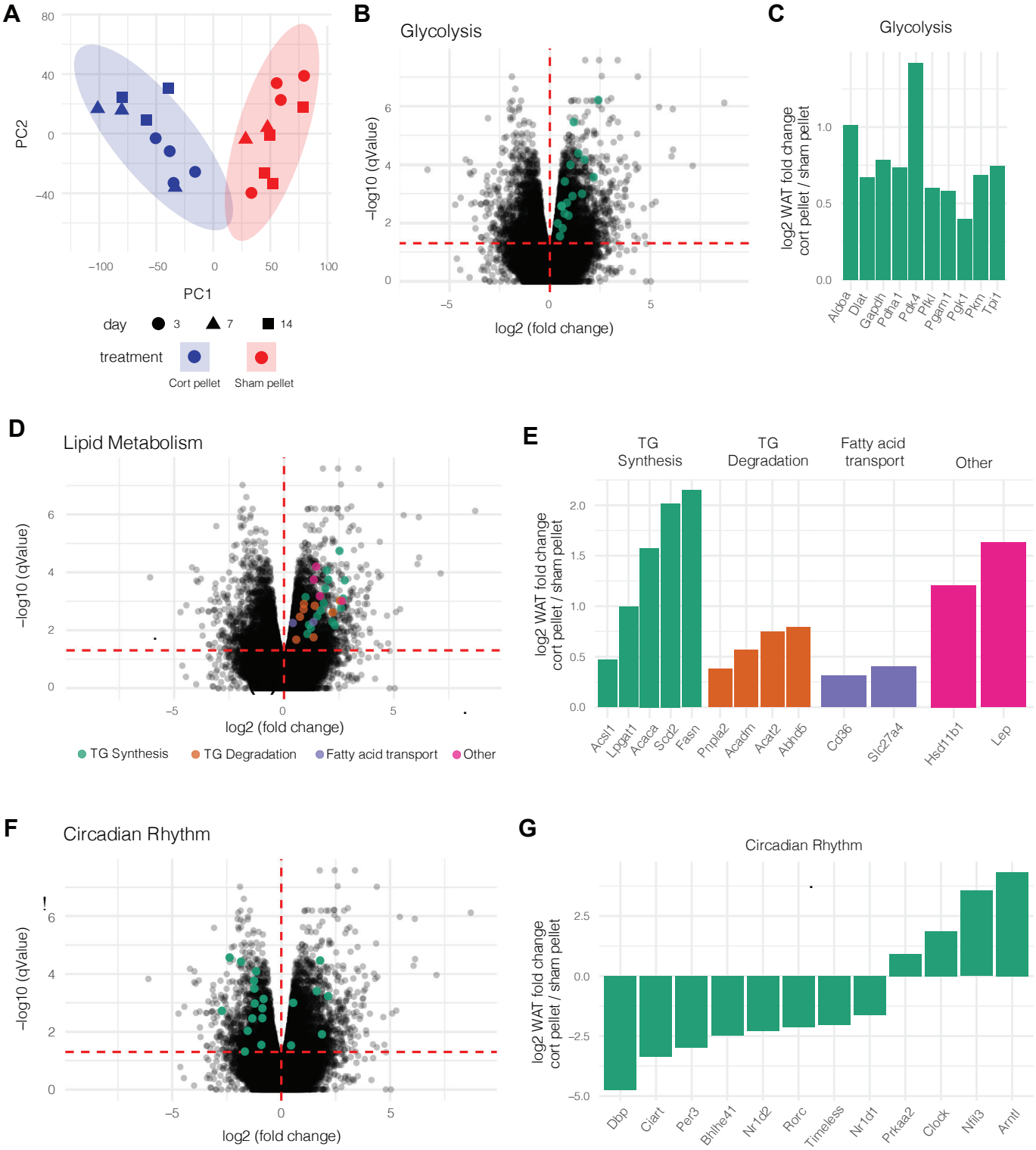

Fig. 6: Flattening of corticosterone oscillations results in gene expression alterations in vWAT of genes involved in glycolysis, lipid metabolism and circadian rhythms. (A) Principal component analysis of vWAT samples from corticosterone and sham pellet implanted mice obtained at 3, 7, and 14 days after pellet implantation. (B-G) Comparison of the vWAT transcriptomes of corticosterone and sham pellet implanted mice. (B-C) Glycolytic genes are highlighted in green. (D-E) Selected genes relevant for lipid metabolism are highlighted in green, orange, purple, and pink. (F-G) Selected genes involved in circadian rhythm are highlighted in green. See also Figure 6-figure supplements 1 and 2 and Figure 6-table supplements 1-3.

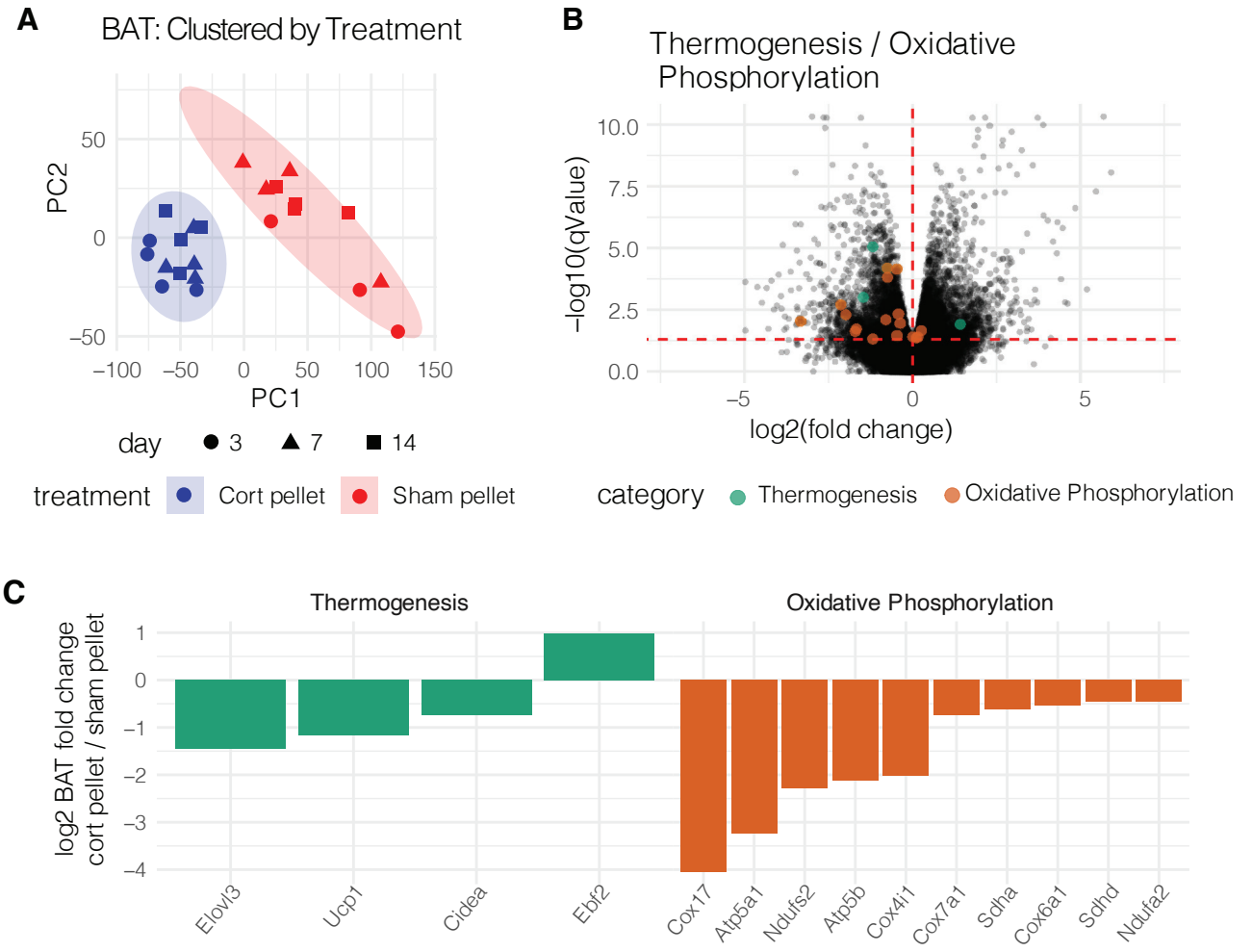

Fig. 7: Flattened corticosterone oscillations in BAT result in altered gene expression of thermogenic genes as well as genes involved in oxidative phosphorylation. (A) Principal component analysis of BAT samples of corticosterone and sham pellet implanted mice 3, 7, and 14 days after pellet implantation. (B) Volcano Plot of all transcripts analyzed comparing BAT of corticosterone and sham pellet implanted mice. Genes related to thermogenesis and oxidative phophorylation (names and log 2 fold changes displayed in figure 7C) are highlighted. (C) Log 2 fold differences of selected thermogenic genes and genes involved in oxidative phosphorylation in BAT of corticosterone and sham pellet implanted mice. See also Figure 7-figure supplements 1 and 2 and Figure 7-table supplements 1 and 2.

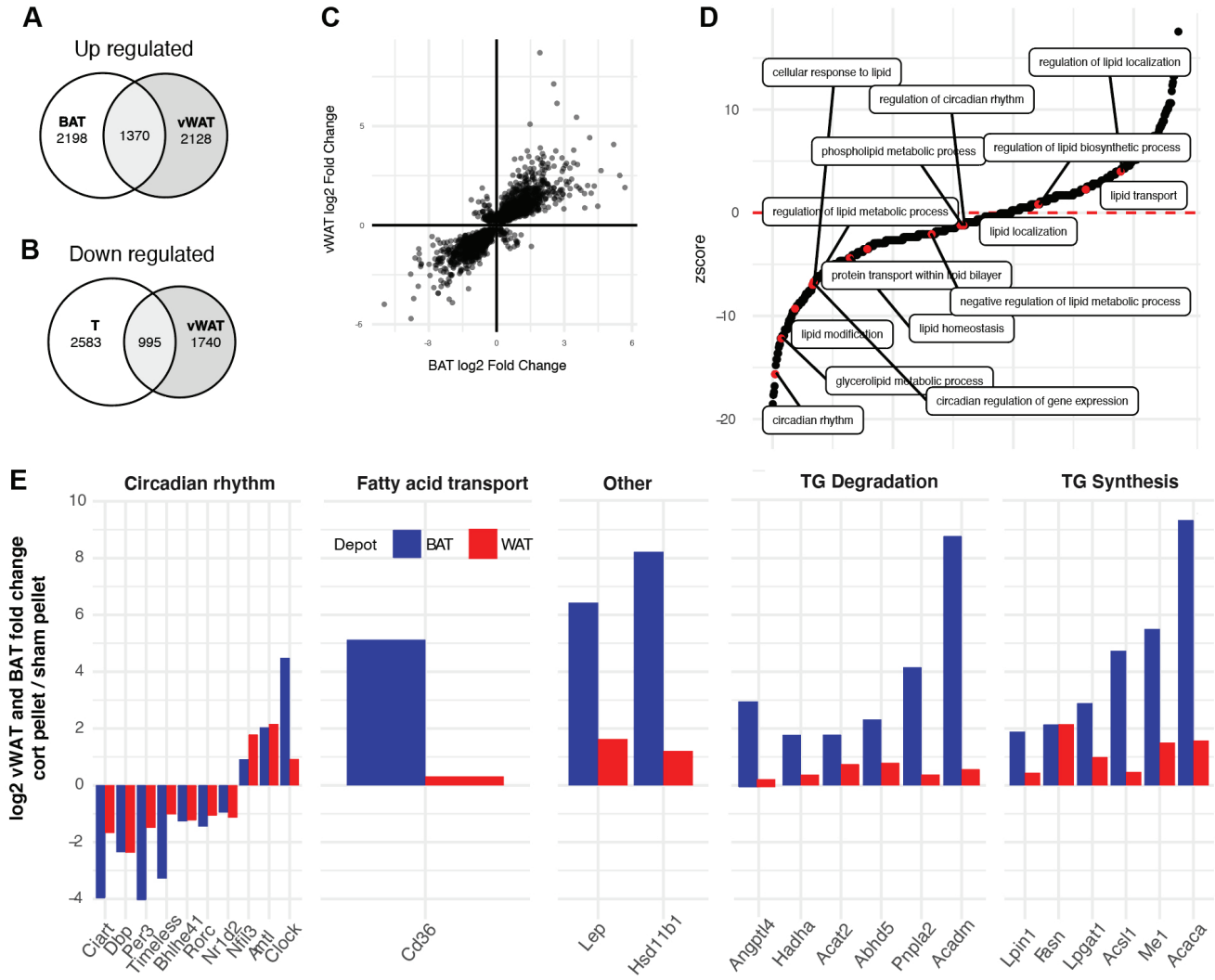

Fig. 8: Transcriptomic analysis of BAT and vWAT upon flattening of corticosterone oscillations reveals similar gene expression alterations of genes involved in lipid turnover. (A/B) Venn diagram showing overlap of genes differently expressed in BAT and vWAT upon flattening of corticosterone oscillations. **(C)** Correlation of log2 fold changes between the vWAT and BAT transcriptomes upon flattening of corticosterone oscillations. **(D)** GO terms positively correlated in WAT and BAT. GO terms related to lipid metabolism are highlighted. **(E)** Log 2 fold changes of selected genes involved in lipid metabolism and circadian rhythms comparing vWAT and BAT upon flattening of corticosterone oscillations.

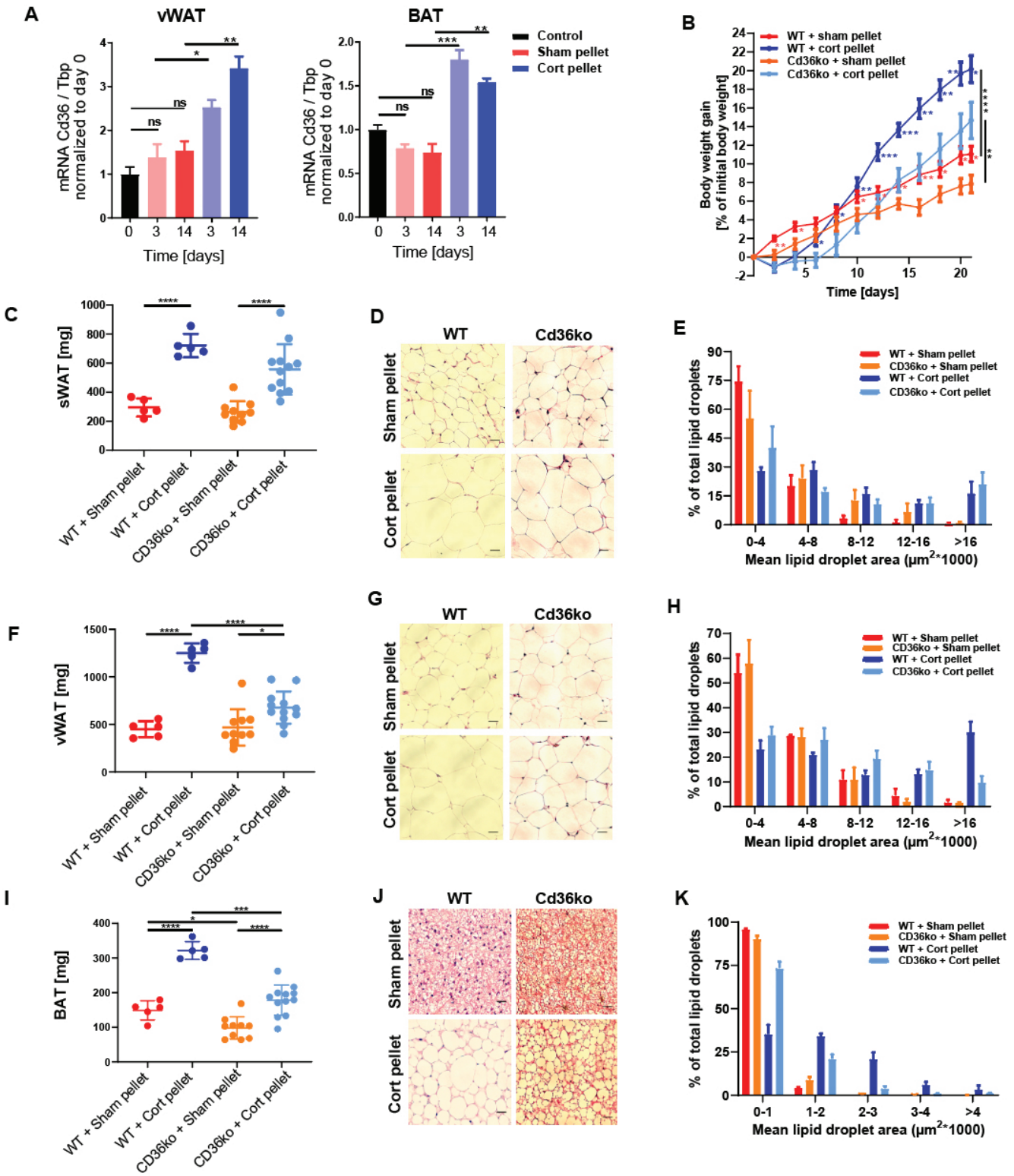

Fig. 9: Cd36ko partially protects against fat gain due to flattening of corticosterone oscillations. (A) mRNA expression for Cd36 measured by qPCR in vWAT and BAT of sham and corticosterone pellet implanted mice 3 and 14 days after implantation. Gene expression data was normalized to the expression of Tbp and is presented as mean ± SEM (n = 3-4). Unpaired t test, *p < 0.05, **p < 0.01, ***p < 0.001, ns = not significant. Control group are mice at start of experiment (day 0). **(B)** Time course showing body weight gain of wild type and Cd36ko mice implanted with corticosterone pellets compared to mice implanted with sham pellets. n = 10-12, mean ± SEM. Unpaired t test (red asterisk: WT + sham pellet versus Cd36ko + sham pellet; blue asterisk: WT + corticosterone pellet versus Cd36ko + corticosterone pellet; black asterisk: sham versus corticosterone pellet), *p < 0.05, **p < 0.01, ***p < 0.001, ****p < 0.0001. **(C)** Weight of epididymal (visceral) fat depots 21 days after pellet implantation, n = 5-12, mean ± SD. Unpaired t test, *p < 0.05, ****p < 0.0001. **(D)** H&E staining of vWAT 21 days after pellet implantation. One representative staining is shown (n = 3-5). Scale bars 50μm. **(E)** Frequency distribution of mean adipocyte area in vWAT as analyzed using Adiposoft (mean + SEM; n=3-5, 25 images per mouse (20x)). **(F)** Weight of inguinal (subcutaneous) fat depots 21 days after pellet implantation, n = 5-12, mean ± SD. Unpaired t test, ****p < 0.0001. **(G)** H&E staining of sWAT 21 days after pellet implantation. One representative staining is shown (n = 4-5). Scale bars 50μm. **(H)** Frequency distribution of mean adipocyte area in sWAT as analyzed using Adiposoft (mean + SEM; n=4-5, 25 images per mouse (20x)). **(I)** Weight of BAT 21 days after pellet implantation, n = 5-12, mean ± SD. Unpaired t test, *p < 0.05, ***p < 0.001, ****p < 0.0001. **(J)** H&E staining of BAT 21 days after pellet implantation. One representative staining is shown (n = 4-5). Scale bars 50μm. **(K)** Frequency distribution of mean adipocyte area in BAT as analyzed using Adiposoft (mean + SEM; n=4-5, 25 images per mouse (20x)). See also Figure 9-figure supplement 1.